NAVAL POSTGRADUATE SCHOOL
Monterey, California

THESIS

PERFORMANCE EVALUATION OF A COOPERATIVE DIVERSITY ENHANCED AD HOC NETWORK

by

Michael A. Tope

December 2002

Thesis Advisor: John C. McEachen
Second Reader: R. Clark Robertson

Approved for public release; distribution is unlimited.

THIS PAGE INTENTIONALLY LEFT BLANK

REPORT DOCUMENTATION PAGE

Form Approved
OMB No. 0704-0188

1. AGENCY USE ONLY *(Leave blank)*	2. REPORT DATE	3. REPORT TYPE AND DATES COVERED
	December 2002	Master's Thesis

4. TITLE AND SUBTITLE :
Performance Evaluation of a Cooperative Diversity Enhanced Ad Hoc Network

5. FUNDING NUMBERS

6. AUTHOR(S)
Tope, Michael A.

7. PERFORMING ORGANIZATION NAME(S) AND ADDRESS(ES)
Naval Postgraduate School
Monterey, CA 93943-5000

8. PERFORMING ORGANIZATION REPORT NUMBER

9. SPONSORING / MONITORING AGENCY NAME(S) AND ADDRESS(ES)

10. SPONSORING /MONITORING AGENCY REPORT NUMBER

11. SUPPLEMENTARY NOTES
The views expressed in this thesis are those of the author and do not reflect the official policy or position of the Department of Defense or the U.S. Government.

12a. DISTRIBUTION / AVAILABILITY STATEMENT
Approved for public release; distribution is unlimited.

12b. DISTRIBUTION CODE

13. ABSTRACT *(maximum 200 words)*

Currently wireless multi-hop ad hoc networks utilize protocols that relay packets of data node-by-node along a path connecting the source node to the sink node. This thesis describes a new methodology called "Cooperative Diversity" where information is relayed from the source to the sink via clusters of neighboring nodes. We first describe a routing protocol to establish spatially diversified paths through a field of randomly dispersed nodes. Second, an idealized configuration called the "Synthetic Waveguide" is introduced and its information theoretic channel capacity is developed. Third, we derive an outage model based channel capacity for the synthetic waveguide operating with a low forwarding latency. The low latency channel capacity is far different from that predicted by traditional channel capacity. Next, a simple modulation called stuttered simulcast is introduced and shown to approach the performance of an optimal distributed space-time code. Finally, a Monte Carlo simulation of the cooperative diversity routing protocol confirms its superior performance in regions of operational interest.

14. SUBJECT TERMS
Wireless, Ad Hoc Network, Synthetic Waveguide, Cooperative Diversity, MIMO, Channel Capacity, Outage Model

15. NUMBER OF PAGES
95

16. PRICE CODE

17. SECURITY CLASSIFICATION OF REPORT	18. SECURITY CLASSIFICATION OF THIS PAGE	19. SECURITY CLASSIFICATION OF ABSTRACT	20. LIMITATION OF ABSTRACT
Unclassified	Unclassified	Unclassified	UL

NSN 7540-01-280-5500

Standard Form 298 (Rev. 2-89)
Prescribed by ANSI Std. 239-18

THIS PAGE INTENTIONALLY LEFT BLANK

Approved for public release; distribution is unlimited.

PERFORMANCE EVALUATION OF A COOPERATIVE DIVERSITY ENHANCED AD HOC NETWORK

Michael A. Tope
B.S.E.E., University of Akron, 1984

Submitted in partial fulfillment of the
requirements for the degree of

MASTER OF SCIENCE IN ELECTRICAL ENGINEERING

from the

NAVAL POSTGRADUATE SCHOOL
December 2002

Author: Michael A. Tope

Approved by: John C. McEachen
Thesis Co-Advisor

Daniel M. Rosser
NSA Co-Advisor

R. Clark Robertson
Second Reader

John P. Powers
Chairman, Department of Electrical and Computer Engineering

THIS PAGE INTENTIONALLY LEFT BLANK

ABSTRACT

Currently wireless multi-hop ad hoc networks utilize protocols that relay packets of data node-by-node along a path connecting the source node to the sink node. This thesis describes a new methodology called "Cooperative Diversity" where information is relayed from the source to the sink via clusters of neighboring nodes. We first describe a routing protocol to establish spatially diversified paths through a field of randomly dispersed nodes. Second, an idealized configuration called the "Synthetic Waveguide" is introduced and its information theoretic channel capacity is developed. Third, we derive an outage model based channel capacity for the synthetic waveguide operating with a low forwarding latency. The low latency channel capacity is far different from that predicted by traditional channel capacity. Next, a simple modulation called stuttered simulcast is introduced and shown to approach the performance of an optimal distributed space-time code. Finally, a Monte Carlo simulation of the cooperative diversity routing protocol confirms its superior performance in regions of operational interest.

THIS PAGE INTENTIONALLY LEFT BLANK

TABLE OF CONTENTS

THIS PAGE INTENTIONALLY LEFT BLANK

LIST OF FIGURES

THIS PAGE INTENTIONALLY LEFT BLANK

LIST OF TABLES

THIS PAGE INTENTIONALLY LEFT BLANK

LIST OF ABBREVIATIONS

ACK	Acknowledgement Frame
AODR	Ad-hoc On-demand Distance Routing
BER	Bit Error Rate
BPSK	Bi-phase Shift Keying
CD	Cooperative Diversity
CDMA	Code Division Multiple Access
CODEAN	Cooperative Diversity Enhanced Ac hoc Network
CRC	Cyclic Redundancy Check
DARPA	Defense Advanced Research Program Agency
DSDV	Destination Sequenced Distance Vector
DSR	Dynamic Source Routing
FDMA	Frequency Division Multiple Access
IP	Internet Protocol
MAC	Multiple Access Channel
MANET	Mobile Ad Hoc Network
MIMO	Multiple Input Multiple Output
MLSE	Maximum Likelihood Sequence Estimator
MRC	Maximal Ratio Combiner
MUD	Multi-User Detection
OSI	Open Systems Interconnection
RF	Radio Frequency
STL	State Transition Logic
SW	Synthetic Waveguide
TDMA	Time Division Multiple Access
TORA	Temporally Ordered Routing Algorithm
TCP	Transport Control Protocol
WLAN	Wireless Local Area Network

THIS PAGE INTENTIONALLY LEFT BLANK

EXECUTIVE SUMMARY

One important goal of communication systems is to establish a point-to-point connection between two end users. Such exchanges typify the telephone system and many computer network transactions such as email and web browsing. Previous and current generations of the systems that provide for such communications are most often based on wired links (including optical fiber). Although Wireless Local Area Network (WLAN) devices and cell phones are common, these systems generally follow the same point-to-point paradigm as found in wired systems. Further, such wireless communications typically traverse only the 'last hop' connecting the mobile user to the wired infrastructure.

Recently, researchers have proposed interconnecting many wireless devices together to form networks based primarily on wireless communications. One obvious application is to reduce the cost in supplying communications to an office building by avoiding the requirement for costly cabling. Others have proposed applications in which numerous miniature sensors are distributed throughout an area of interest, and these sensors collaborate exchanging information via wireless links. For example, the Defense Advanced Research Program Agency (DARPA) is developing sensors to scatter throughout a combat area. If an enemy vehicle is detected, the sensors could organize and construct a temporary communication-forwarding path, hopping data from one sensor to another like a game of leapfrog to move the detection data to a field commander for appropriate action.

The wired network paradigm impedes development of these wireless-networking applications because wired networks are built upon highly reliable individual communication links. In contrast, wireless communications are inherently unreliable due to RF propagation effects. For example, in early telephone systems a series of trunk line pairs interconnecting various exchange points were chosen and dedicated to connect the communicants throughout the duration of the communication session. Any failure along this communication path would disrupt the end-to-end communications, so system engineers strived to create highly reliable wired components. This methodology persists today in most modern networks including computer networks and cellular networks.

In this thesis, a new approach to wireless network communications is described that leverages the fact that RF energy scatters and propagates to many users simultaneously. Using the protocol and modulation techniques developed within this thesis, numerous individual users could cooperate together to the mutual benefit of all via the Cooperative Diversity (CD) methodology. Specifically, this thesis describes and evaluates a protocol designed to establish end-to-end communication within a large field of autonomous wireless devices with reduced latency and greatly increased robustness against signal fading and interference. In addition, this new protocol often requires less transmit power than existing techniques.

Variations on the Cooperative Diversity methodology should be applicable to a wide array of wireless communication system and architectures.

THIS PAGE INTENTIONALLY LEFT BLANK

I. INTRODUCTION

The role of wireless communication is expanding. Both the recent ability to manufacture low cost complex wireless transceivers and the inherent mobility of wireless devices have allowed wireless communication to quickly replace many traditionally wired telecommunication devices. While currently wireless devices are typically found only at the 'last communication hop' between the end user and the wired network (such as in current cellular systems and Wireless Local Area Networks (WLANs) [1]), researchers plan to develop wireless routers and other equipment to support large entirely wireless-based installations. Further, some researchers [2] are envisioning many new applications involving the self-organization and collaboration among numerous autonomous semi-intelligent wireless devices. Scattering a large number of such devices over an area could provide crop/soil monitoring, traffic flow analysis, etc. The ability of such wireless devices to establish reliable communication is the focus of this thesis.

Currently proposed wireless multi-hop ad hoc networks or mobile ad hoc networks (MANETs) use one of a variety of routing protocols that operate very similarly to wired networks. Various wireless links are considered to connect pairs of nodes in a point-to-point manner and routing protocols typically behave as if a 'wired' connection allowed reliable bi-directional communication to exist among neighboring pairs of nodes throughout the network [3].

This tradition likely arises from the widely accepted Open Systems Interconnections (OSI) model [4] that layers the services and responsibilities required for network communications in order to promote interoperability among various implementations. The physical layer and the data-link layer are assumed to provide such reliable point-to-point communication between various devices within the network. The network layer interfaces with the data-link layer to establish a communication route to transverse across the various devices comprising the network.

Unfortunately, individual wireless communications links are inherently unreliable because RF propagation effects such as fading, shadowing, and interference can frequently disrupt wireless communication [1]. Further, RF energy cannot easily be directed to a specific single individual receiver node (using current technologies). Typically, RF energy scatters and diffracts throughout a complex environment creating interference on adjacent communication paths. This thesis develops a new methodology called Cooperative Diversity (CD) that leverages these characteristics of wireless RF

propagation to increase the overall communication reliability within similar cost constraints as traditional techniques.

A. BACKGROUND

This section describes the general problem of communication across a wireless Multi-hop Ad Hoc Network or Mobile Ad Hoc Network (MANET) and the general formulation of the Cooperative Diversity approach.

The communication environment of the MANET is an area in which some number of relay nodes or transceivers are randomly dispersed (see Figure 1). These relay nodes are autonomous devices that can send and receive signals in such a way to form a wireless network throughout this area.

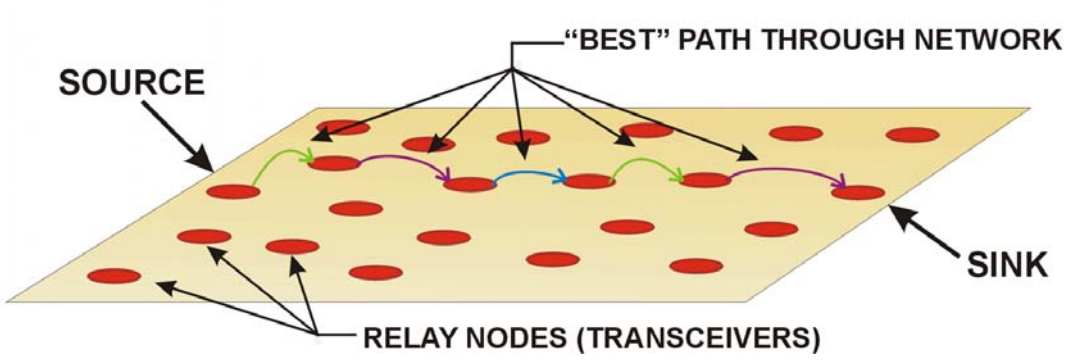

Figure 1. Conventional Cooperative Diversity Cellular Network

The process of establishing a unidirectional link from a communications source node to a remote communications sink node is traditionally accomplished by finding the best single path through the field of relay nodes. Packets of data are hopped from one relay to the next along this best path toward the communication sink.

Throughout this thesis, the relay nodes are assumed to be in relatively fixed positions for the duration of the communication transaction between the source node and the sink node. Individual nodes may move to the degree that induces significant fading changes, but the possibility of continuously adding and/or removing various moving relay nodes to an active in-place communication route is not accommodated. Even for fixed nodes, the quality of individual communication links between neighboring nodes can vary significantly over time [1].

In such a fading environment, the single best path connecting the source node to the sink node becomes dynamic. The movement of RF obstacles or interference within the environment could suddenly and significantly degrade one or more hops or relay

links and interrupt end-to-end communication until a new suitable communication path is discovered (see Figure 2).

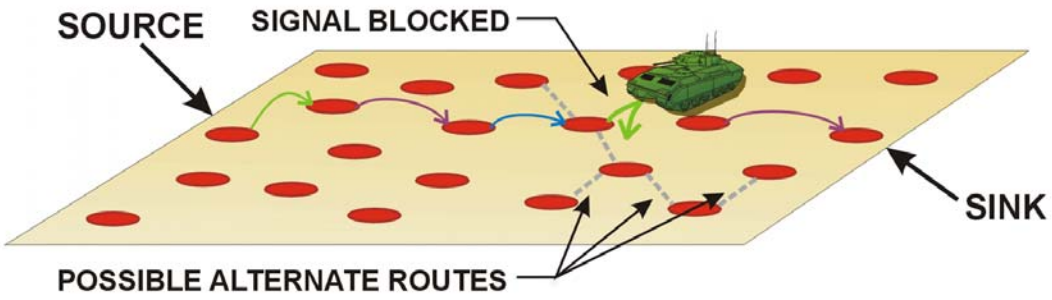

Figure 2. Dynamic Routing in Fading Environment

One method to combat this is to use dispersity routing [5], where several separate parallel paths through the network simultaneously and redundantly carry the information from the source node to the sink node (see Figure 3). This creates spatial diversity to sustain the communication flow even though some relay links may fade or fail. Unfortunately, dispersity routing requires additional bandwidth to prevent self-interference or crosstalk among the independent communication channels forming the end-to-end communication route.

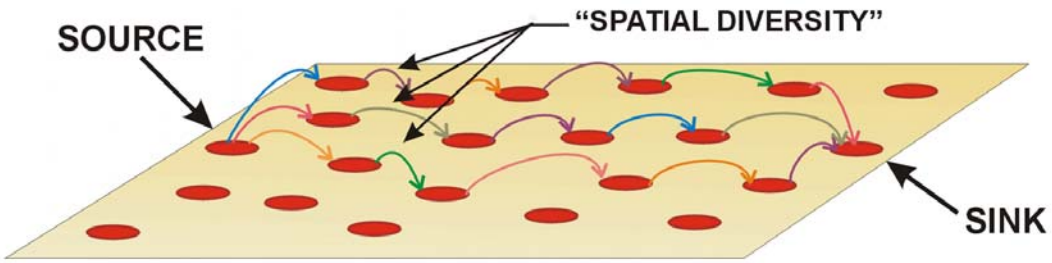

Figure 3. Dispersity Routing

The Cooperative Diversity (CD) solution forms logical clusters or groups of relay nodes and hops information packets from cluster to cluster rather than from individual relay node to relay node (see Figure 4). As in dispersity routing, cooperative diversity creates spatial diversity to increase robustness against channel fading. In dispersity routing, redundant information is combined only at the sink node, but in cooperative diversity spatially distributed information is recombined at every hop via transmit diversity. All the paths between adjacent clusters must fail in order to disrupt end-to-end communication.

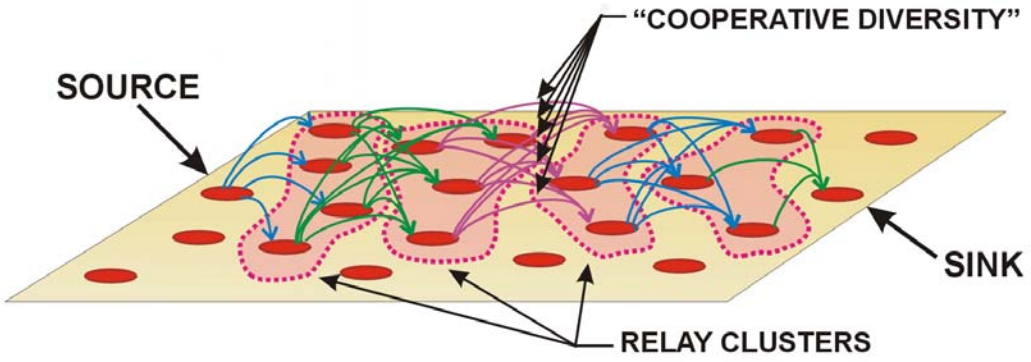

Figure 4. Cooperative Diversity Routing

From a quick glance comparing the traditional routing approach in Figure 1 to the cooperative diversity approach in Figure 4, we see that the cooperative diversity depiction involves many more nodes in the communication path from the source to the sink. For an equitable comparison, the cooperative diversity approach must be restricted to the same number of nodes and the same number of signal transmissions as a conventional ad hoc network. For a given number of relay nodes, the performance metric will be the minimal required transmit power per relay node to close the link from the source node to the sink node (with high probability) in a fading environment.

Typically, ad hoc network researchers model the random position of each relay node within the ad hoc network environment as independently and identically distributed according to a two-dimensional uniform Poisson random variable. Such a model typically requires intractable stochastic geometric methods to formulate an analytical solution. As a result most ad hoc network performance analysis is usually conducted using Monte Carlo simulations.

In this thesis, the performance of a cooperative diversity enhanced ad hoc network shall be predicted by introducing a simplified topology called the Synthetic Waveguide (SW) (see Figure 5). After the ad hoc network routing protocol has set up the communication path from the source node to the destination node, the selected nodes along the communication path are moved to equidistant spaced points along a line connecting the source node and the destination node. Traditional ad hoc network routing approaches are approximated by the bucket brigade, which can be considered a cooperative diversity network with only one node per cluster. As the number of nodes per cluster increases, so does the distance between clusters of nodes, so that the total number of nodes involved in the communication path is constant regardless of the cluster size.

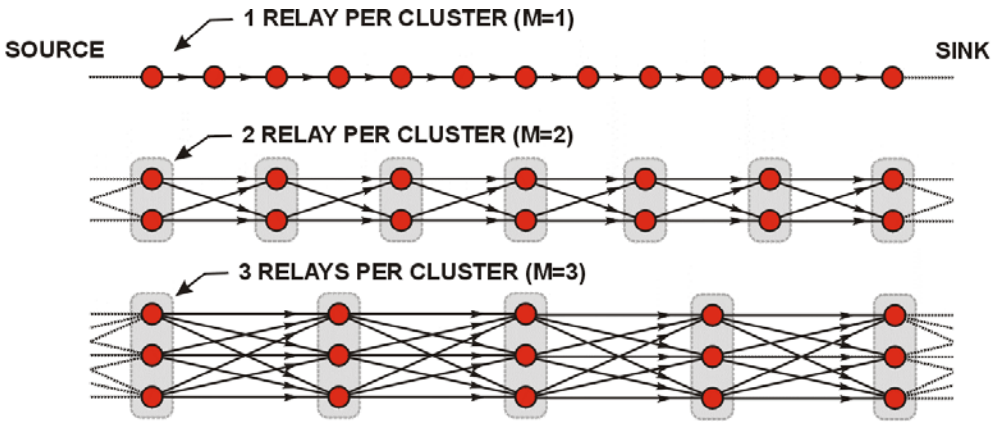

Figure 5. Various Synthetic Waveguide Configurations

B. OBJECTIVE

The first objective of this thesis is to evaluate and characterize the communication performance advantage (if any) that results from incorporating Cooperative Diversity into a multi-hop ad hoc network. This evaluation is conducted using the simplifying Synthetic Waveguide structure.

The second objective is to develop and describe an ad-hoc network protocol that creates a cooperative diversity enhanced route through an ad hoc network. This Co-Operative Diversity Enhanced Ad hoc Network (CODEAN) protocol strives to select relay nodes and form a communication route resembling the synthetic waveguide model.

The final objective is to compare the results of a Monte Carlo simulation of the CODEAN protocol with the analytical results derived for the synthetic waveguide.

C. RELATED WORK

Various researchers have developed a large number of protocols for routing communication within ad hoc networks including the Ad-hoc On-demand Distance Routing (AODR) protocol [3], the Temporally Ordered Routing Algorithm (TORA) [6, 7], the Dynamic Source Routing (DSR) protocol [8], and the Destination Sequenced Distance Vector (DSDV) routing protocol [9]. All of these protocols operate at the network layer within the OSI model.

The cooperative diversity concept was first described by the author and applied to a cellular communication system in [10] (see Figure 6). In this scheme, nearby cell phones share information effectively forming virtual antenna arrays to combat channel fading. The results of a simple Monte Carlo simulations demonstrated that a cooperative

diversity approach could allow current sectorized cellular phone system architectures to support three to six times more mobile subscriber units.

Preliminary results on the performance of the synthetic waveguide were reported in [11] and [12].

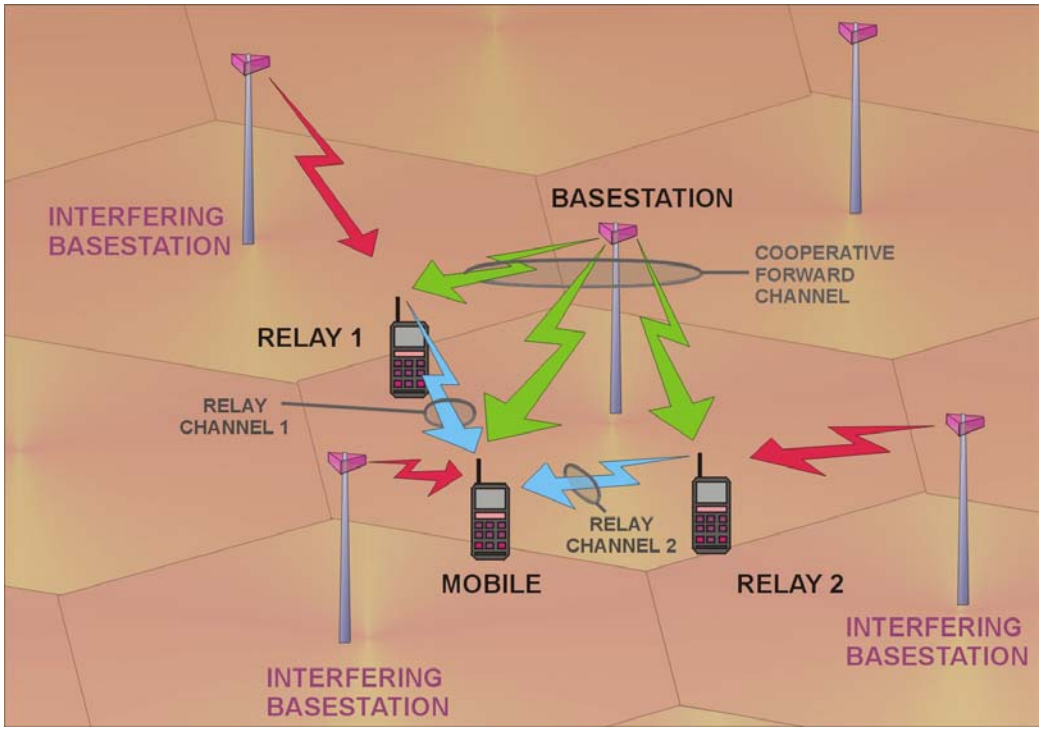

Figure 6. Cooperative Diversity Cellular Network

D. THESIS ORGANIZATION

This chapter provides background information including a description of the role of Cooperative Diversity (CD) in ad hoc networking. The objectives of this thesis are also presented along with a brief survey of related ad hoc networking protocols.

In Chapter II, the Co-Operative Diversity Enhanced Ad hoc Network (CODEAN) is described. The goal of this routing protocol is to setup a communications route through a field of randomly dispersed relay nodes that approximates the topology of the synthetic waveguide.

In Chapter III, the information theoretic channel capacity of the synthetic waveguide is determined for two modes of operations. The first mode of operation is where the source information must be distributed to every node participating in the

synthetic waveguide. The second mode of operation strived to simply deliver the source information to the sink node.

In Chapter IV, the channel capacity of a low-latency synthetic waveguide using an outage model is determined. For the low latency synthetic waveguide, the relays must immediately forward packets upon reception. Three modes of modulation are examined including a novel method called "stuttered simulcast." Finally, using Monte Carlo simulations, the performance of the CODEAN protocol is estimated and compared to the theoretical performance of the synthetic waveguide.

THIS PAGE INTENTIONALLY LEFT BLANK

II. THE CODEAN PROTOCOL

This chapter describes the Co-Operative Diversity Enhanced Ad hoc Networking (CODEAN) protocol, which is loosely based on the Ad-hoc On-demand Distance-vector Routing) AODR protocol [3]. The purpose of this protocol is to establish a communication route between the source node and the sink node that approximates the idealized Synthetic Waveguide (SW) within the field of randomly dispersed relay nodes.

The CODEAN protocol is quite minimal. For example, every node is assumed to possess a globally unique identifier, and a source node must know the identifier of a destination node in order to establish a link to it. No mechanism is provided to query the network for a given node that has specific information of interest. The primary purpose of this protocol is to establish a route suitable to drive the Monte Carlo simulations in order to estimate the end-to-end communication performance.

The CODEAN protocol selects a route that strives to use the fewest number of hops to connect the source node to the destination nodes. This is accomplished using the fading conditions arising at the moment that the route is formulated. The protocol does not repeatedly ping various links to discover the average link quality. Further, the transmission of information to a neighboring node is not acknowledged; however, given the end-to-end redundancy created by this protocol, the occasional loss of a node is not significant.

The CODEAN protocol includes five message types (see Table 1):

- ROUTE_REQUEST
- ROUTE_REPLY
- CLUSTER_PROBE
- PROBE_REPLY
- CLUSTER_ACK; and
- DATA

The first two messages – ROUTE_REQUEST and ROUTE_REPLY – are used in the initial router discovery phase. The next three messages – CLUSTER_PROBE, PROBE_REPLY, and CLUSTER_ACK – are used in the cluster formation phase. Finally, messages of type DATA are used to transfer information.

Message Type	Description
ROUTE REQUEST	Initiated by the source node and forwarded by intermediate relays nodes to setup a communication route through the ad hoc network to a given sink (or destination) node.
ROUTE REPLY	Initiated by the sink node upon reception of a ROUTE_REQUEST and forwarded by intermediate relays node to finalize the selection of the communication route through the ad hoc network allowing communication to flow from the source node to the sink node.
CLUSTER PROBE	Sent by cluster leader nodes along the communication route to seek neighboring nodes suitable to join the cluster.
PROBE REPLY	Sent by neighboring nodes in response to a CLUSTER_PROBE to describe their routing state to the cluster leader.
CLUSTER ACK	Sent by the cluster leader to select specific nodes to join its cluster.
DATA	Initiated by the source node and forwarded by intermediate relays node to deliver information to the sink node.

Table 1. Description of CODEAN Protocol Message Types

The general operation of the CODEAN protocol is to establish a route from a source node to the sink node as illustrated in Figure 7 and Figure 8. The gray lines in these figures reflect the RF connectivity among various nodes during the illustrated route set-up.

The CODEAN protocol's operation begins with the source node, which seeks to establish a communication link to the sink node, broadcasting a ROUTE_REQUEST message to its immediate neighbors. Each relay node that receives the ROUTE_REQUEST message consults its routing database to see if this particular ROUTE_REQUEST was already processed and, if not, the ROUTE_REQUEST message is updated and retransmitted. The ROUTE_REQUEST message from the source node propagates across the field of relay nodes until reaching the sink node (see Figure 7).

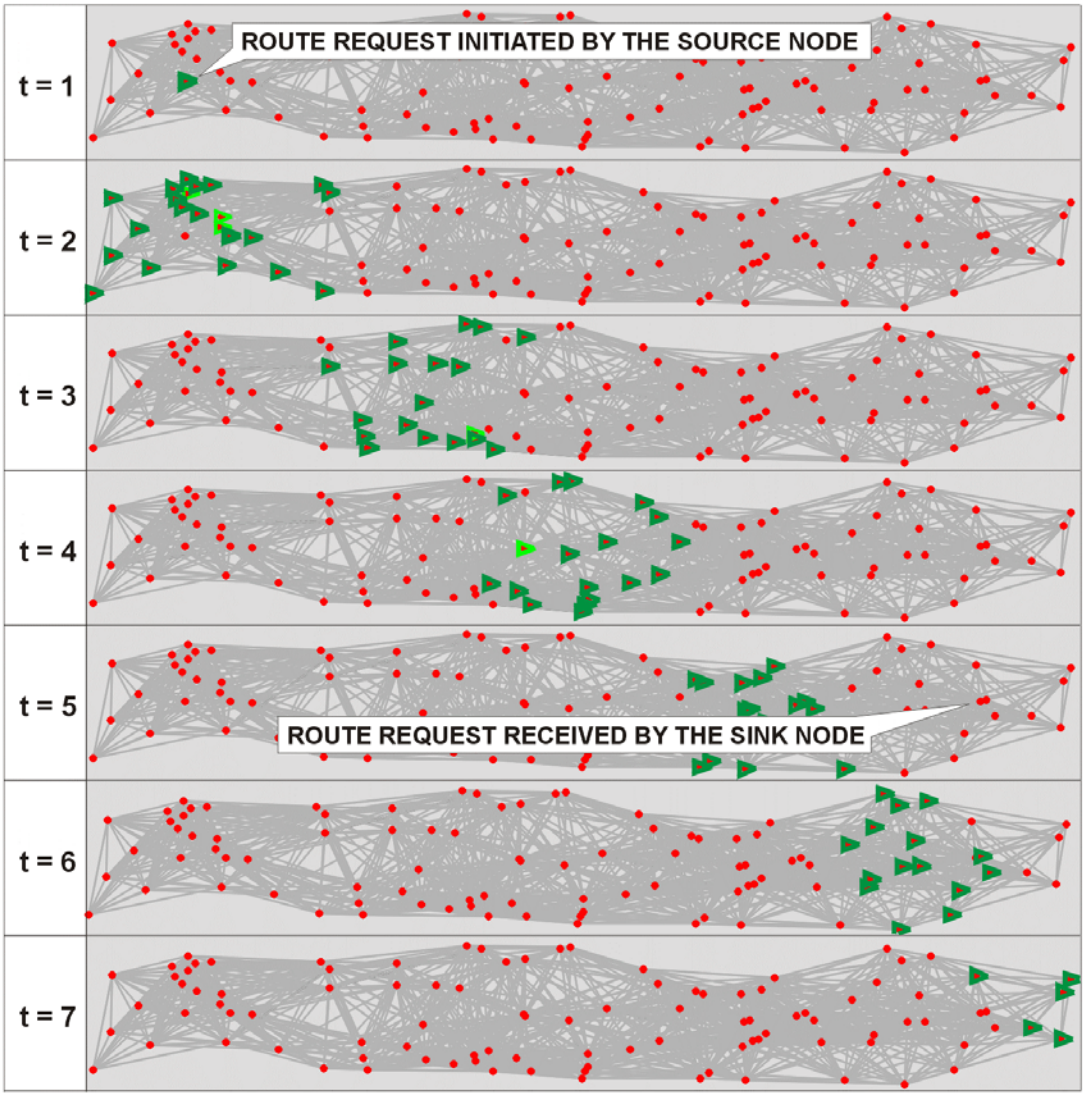

Figure 7. Route Setup Forward Messaging

The sink node then sends a ROUTE_REPLY message addressed to the specific neighboring node that first delivered the ROUTE_REQUEST message (see Figure 8). This single neighboring node consults its routing database and likewise selects the node that first delivered the same ROUTE_REQUEST message to it. The process continues to backtrack the ROUTE_REPLY message through the network towards the source node.

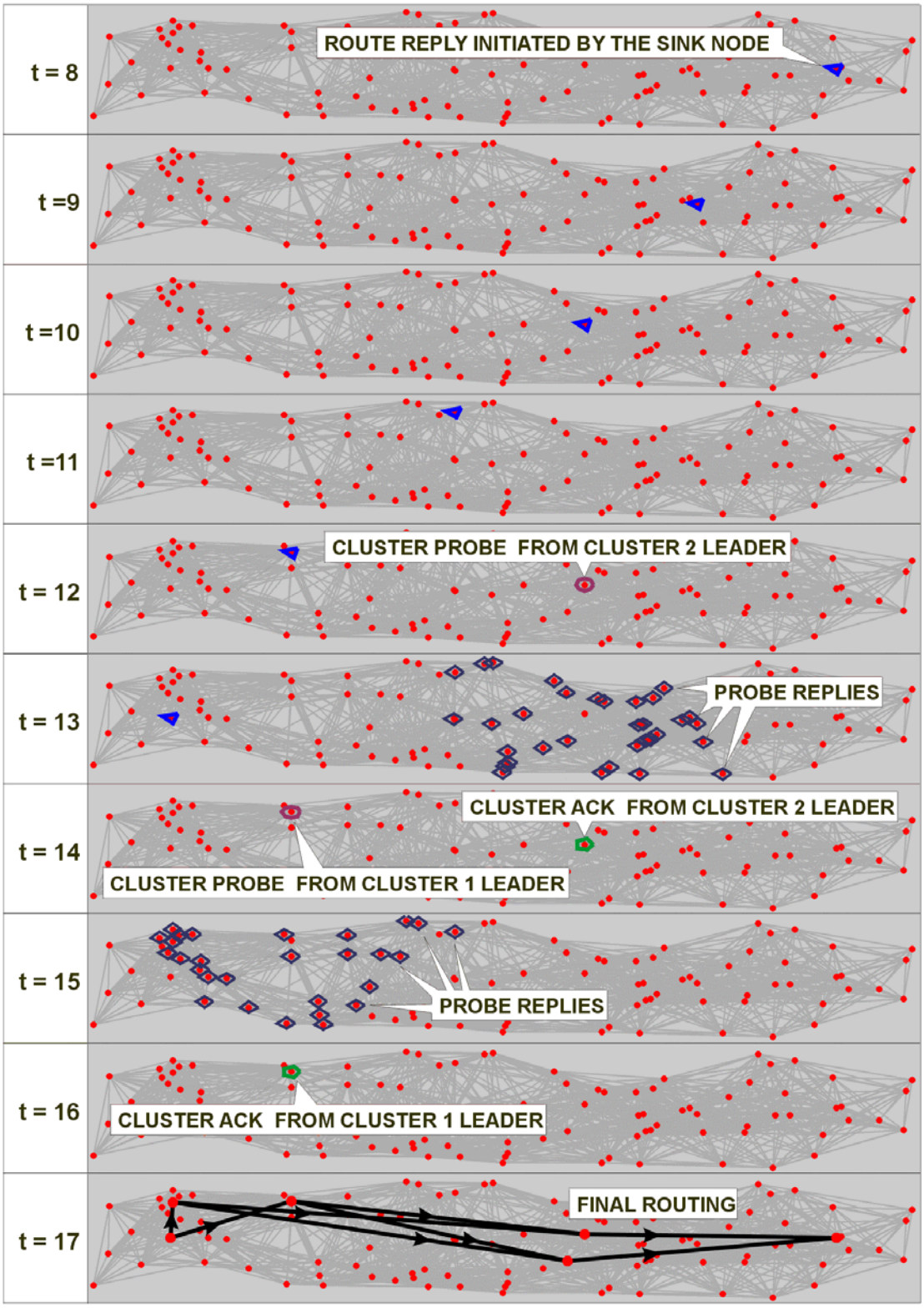

Figure 8. Route Setup Reverse Messaging

In addition, each relay receiving a ROUTE_REPLY message addressed to it also notes its position along the communication path, and every M^{th} node elects itself as the cluster leader (where M is the cluster size). Each cluster leader sends a CLUSTER_PROBE message to query the status of the neighboring nodes. These neighboring nodes respond with a PROBE_REPLY message containing route status information. The cluster leader uses this route state information to select the $(M - 1)$ most appropriate neighboring nodes to join the cluster. The cluster leader sends each of these selected nodes a CLUSTER_ACK message. The route from the source node to the sink node is now set (see the $t = 17$ frame in Figure 8).

Now that the route is set, the source node may forward message data to the sink node. Whenever the source node transmits a packet of data, each relay node that can demodulate the transmission consults its routing database. If a given node is a member of the cluster scheduled to propagate the message toward the destination, it updates and retransmits the DATA message. Note that all of the relay nodes in a given cluster transmit simultaneously.

Each relay node within the field must maintain a database listing the routes for which it is an active participant. The information pertaining to a given route is indexed by the source and sink identifiers, and the routing specification associated with this index is described in Table 2.

Field	Description	Comments
RoutingState	Routing State – the State of this Routing Specification within the protocol's State Transition Logic (STL).	States include: REQUEST_PENDING, PROBE_ACTIVE, ROUTE_SET, "UNSET"
SrcNodeID	Source Node Identifier – the ID of the node initiating the communication and possessing information to distribute to the sink node.	Every node within the environment must have a unique ID.
SnkNodeID	Sink Node Identifier – the ID of the node to ultimately receive information from the source node.	
BroadcastID	Broadcast Message Identifier – the ID used to associate a given relayed message from the source node throughout the network	The source node should increment this ID with each message sent.
NeighborID	Neighboring Node Identifier – the ID of the neighboring node from which this routing spec was derived via a ROUTE REQUEST message.	
FwdHopCnt	Forward Hop Count – the number of hops from the source node to this node.	
RevHopCnt	Reverse Hop Count – the number of hops from this node to the sink node.	
ClusterSize	Cluster Size – the number of nodes sought to form each cluster.	
LeaderFlag	Cluster Leader Flag – indicated whether or not this node is a cluster leader.	
MemberNum	Cluster Member Number – identifies the node within a given cluster.	Used with Cluster Leader Node ID to form a globally unique ID.

Table 2. Routing Specification

The routing specification is present in one of the four states described in Table 3, and the transition from state to state is illustrated in Figure 9.

The ROUTE_REQUEST message floods the entire field of relay nodes; therefore, every node enters a routing specification into its routing database for every ROUTE_REQUEST. If the node is not selected to join a cluster within a set amount of time, the routing specification is deleted and the effective state of the route becomes "UNSET."

Message Type	Description
"UNSET"	No routing specification exists for the route from the source node to the sink node.
ROUTE PENDING	Received a ROUTE_REQUEST message and created an associated routing specification, and now awaiting a ROUTE_REPLY or CLUSTER_ACK message in order to become an active participant in forwarding data along this route.
PROBE_PENDING	Selected as the cluster leader, and now currently awaiting for responses to the CLUSTER_PROBE messages.
ROUTE_SET	Selected to as a member of the route to forward data from the source node to the sink node.

Table 3. Description of CODEAN Routing States

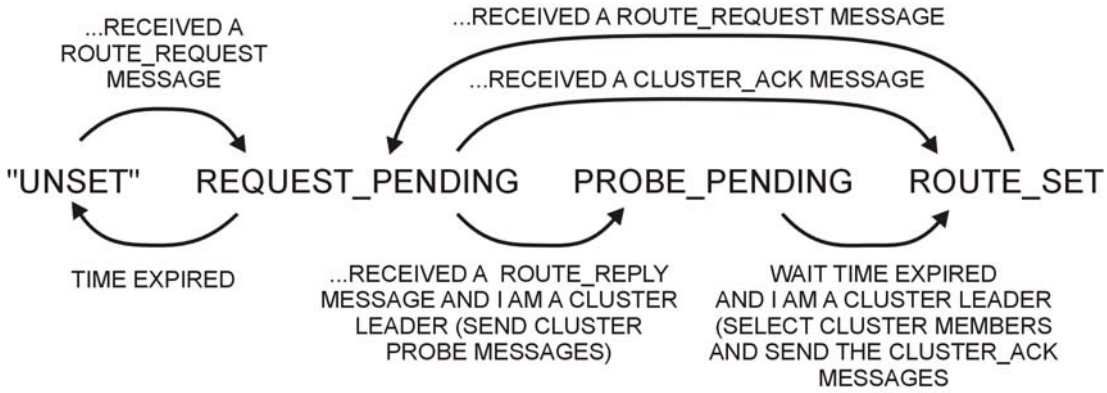

Figure 9. State Transition Logic Flowchart

Each relay node that received a ROUTE_REPLY message addressed to it determines whether or not it is the cluster leader using Equation (1). The source node has a hop count of zero, so a node that is the immediate neighbor the source node will always be chosen as a cluster leader.

$$\text{if}(\mathit{FwdHopCnt} \bmod \mathit{ClusterSize} == 1) \text{ then a cluster leader} \quad (1)$$

Selection of the cluster leader and other members of the first cluster from the set of relay nodes in the immediate vicinity of the source node ensures the reliable transfer of information from the source node into the first cluster.

The fields contained with the ROUTE_REQUEST message are described in Table 4. The XmitNodeID field is always set to the identifier of the transmitting node. The descriptions of the fields for the ROUTE_REPLY message are listed in Table 5.

Field	Description	Comments
SrcNodeID	Same as in the Routing Specification (see Table 2).	Constant throughout route set-up process.
SnkNodeID	Same as in the Routing Specification (see Table 2).	Constant throughout route set-up process.
BroadcastID	Same as in the Routing Specification (see Table 2).	Constant throughout route set-up process.
FwdHopCnt	The number of hops from the source node.	Increments as the ROUTE_REQUEST traverses away from the source node.
ClusterSize	Same as in the Routing Specification (see Table 2).	Constant throughout route set-up process.
XmitNodeID	Transmit Node Identifier – the ID of the node that transmits this message.	Set to the node ID of the node transmitting the message.

Table 4. ROUTE_REQUEST Message

Field	Description	Comments
SrcNodeID	Same as in the Routing Specification (see Table 2).	Constant throughout route set-up process.
SnkNodeID	Same as in the Routing Specification (see Table 2).	Constant throughout route set-up process.
BroadcastID	Same as in the Routing Specification (see Table 2).	Constant throughout route set-up process.
FwdHopCnt	The number of hops from the source node.	Decrements as the ROUTE_REPLY traverses back towards the source node.
RevHopCnt	The number of hops from the sink node.	Increments as the ROUTE_REPLY traverses back towards the source node.
AckNodeID	Acknowledgement Node Identifier – the ID of the single neighboring node which should respond to this ROUTE_REPLY.	Set to the NeighborID recorded within the routing specification.

Table 5. ROUTE_REPLY Message

The CLUSTER_PROBE message (see Table 6) is sent by each cluster leader to query for neighboring relay nodes that are available to join the cluster. The PROBE_REPLY message (see Table 7) is sent back to the cluster leader by those neighboring nodes that both hear the CLUSTER_PROBE and have not already joined a cluster.

Field	Description	Comments
SrcNodeID	Same as in the Routing Specification (see Table 2).	Constant throughout route set-up process.
SnkNodeID	Same as in the Routing Specification (see Table 2).	Constant throughout route set-up process.
BroadcastID	Same as in the Routing Specification (see Table 2).	Constant throughout route set-up process.
XmitNodeID	Transmit Node Identifier – the ID of the node that transmits this message.	

Table 6. CLUSTER_PROBE Message

Field	Description	Comments
SrcNodeID	Same as in the Routing Specification (see Table 2).	Constant throughout route set-up process.
SnkNodeID	Same as in the Routing Specification (see Table 2).	Constant throughout route set-up process.
BroadcastID	Same as in the Routing Specification (see Table 2).	Constant throughout route set-up process.
FwdHopCnt	The number of hops from the source node.	Set to the value stored within the transmitting nodes routing specification.
RevHopCnt	The number of hops from the sink node.	Set to the value stored within the transmitting nodes routing specification.
AckNodeID	Acknowledgement Node Identifier – the ID of the single neighboring node which should respond to this PROBE_REPLY.	Node ID of the cluster leader that sent the CLUSTER_PROBE message for which this reply is associated.
XmitNodeID	Transmit Node Identifier – the ID of the node that transmits this message.	

Table 7. PROBE_REPLY Message

After all PROBE_REPLY messages arrive at the cluster leader, the cluster leader selects the top nodes to form the cluster and sends each one of then a CLUSTER_ACK message as described in Table 8. The criteria for selection are listed in Table 9. The goal of the selection criteria is to select nodes close to the cluster node and located near a line that is both perpendicular to the direction of the communication and intersecting the cluster node. If a neighboring node has the same forward hop count, then that node is likely a good candidate to join the cluster. Next, try to use nodes whose forward hop count differs by a value of one; otherwise, use any node available. This protocol could likely be improved by including measured signal link quality information in the PROBE_REPLY message to improve the cluster leader's selection process.

Field	Description	Comments
SrcNodeID	Same as in the Routing Specification (see Table 2).	Constant throughout route set-up process.
SnkNodeID	Same as in the Routing Specification (see Table 2).	Constant throughout route set-up process.
BroadcastID	Same as in the Routing Specification (see Table 2).	Constant throughout route set-up process.
FwdHopCnt	The number of hops from the source node.	Set by the cluster leader.
RevHopCnt	The number of hops from the sink node.	Set by the cluster leader.
AckNodeID	Acknowledgement Node Identifier – the ID of the single neighboring node which should respond to this CLUSTER_ACK.	Set to the node ID of selected cluster nodes by the cluster leader.
MemberNum	Same as in the Routing Specification (see Table 2).	Set by the cluster leader.

Table 8. CLUSTER_ACK Message

Message Type	Description
PRIMARY	Choose those nodes whose routing specifications have the same FwdHopCnt as the cluster leader (these nodes to lie near the cluster leader and perpendicular to the direction of the communication route.
SECONDARY	Choose those nodes whose routing specifications have the nearly the same FwdHopCnt (off by a count of one).
TERTIARY	Choose any node that replied to the CLUSTER_PROBE

Table 9. Cluster Selection Criteria

Details pertaining to message processing are described in Table 10 using a C programming language pseudo-code description.

On Reception of a Message of this MessageType	Description of Message Processing

ROUTE_REQUEST	Search the routing database for a routing specification that matches the {SrcNodeID, SnkNodeID, and BroadcastID} of this message;
	IF (no such routing specification is found)
	{
	Create a new routing specification using the information received in the ROUTE_REQUEST message (set the Routing State to ROUTE_PENDING);
	
	IF ('this' node is not the sink node)
	{
	Forward this ROUTE_REQUEST with an incremented FwdHopCnt;
	}
	ELSE
	{
	Send a ROUTE_REPLY with the AckNodeID set to the XmitNodeID of this ROUTE_REQUEST message and with the RevHopCnt set to zero;
	}
	}

ROUTE_REPLY	Search the routing database for a routing specification that matches the {SrcNodeID, SnkNodeID, BroadcastID, and FwdHopCnt} of this message
	IF (such a routing specification is found, and its Routing State set to ROUTE_PENDING)
	{
	Forward this ROUTE_REQUEST with an incremented RevHopCnt, a decremented FwdHopCnt, and the AckNodeID set to the node listed in the routing specification (the XmitNodeID);
	
	IF (the hop counts indicate that 'this' node is a Cluster Leader – see Equation (1))
	{
	Send a CLUSTER_PROBE, and set the routing state to PROBE_PENDING
	}
	}

CLUSTER_PROBE	Search the routing database for a routing specification that matches the {SrcNodeID, SnkNodeID, and BroadcastID} of this message;
	IF (such a routing specification is found and its Routing State not set the ROUTE_SET)
	{
	Send a PROBE_REPLY set according to the routing specification, and with the AckNodeID set to the XmitNodeID that sent the CLUSTER_PROBE;
	}

PROBE_REPLY	Search the routing database for a routing specification that matches the {SrcNodeID, SnkNodeID, and BroadcastID};
	IF (such a routing specification is found, its Routing State is set the PROBE_PENDING, and the AckNodeID field is the same as 'this' node's ID)
	{
	Add the information within the PROBE_REPLY message to the list used to select those nodes within this cluster;
	After a period of time expires, select the other nodes within this cluster (using the criteria in Table 9) and send them CLUSTER_ACK messages;
	}

CLUSTER_ACK	Search the routing database for a routing specification that matches the {SrcNodeID, SnkNodeID, and BroadcastID} of this message;
	IF (such a routing specification is found, its Routing State not set to ROUTE_SET, and the AckNodeID field is the same as 'this" node's ID)
	{
	Update the FwdHopCnt, RevHopCnt and MemberNum fields of the routing specification to match those received in the CLUSTER_ACK message;
	Set the RoutingState to ROUTE_SET;
	}

DATA	Search the routing database for a routing specification that matches the {SrcNodeID, SnkNodeID, FwdHopCnt, and RevHopCnt} of this message;
	IF (such a routing specification is found, and the RoutingState is equal to ROUTE_SET)
	{
	IF (FwdHopCnt is one)
	{
	Forward the DATA message to the next cluster

	with an incremented the FwdHopCnt and
	decremented RevHopCnt;
	}
	ELSE
	{
	Forward the DATA message to the next cluster
	with FwdHopCnt increased by the ClusterSize,
	and the RevHopCnt decreased by the
	ClusterSize;
	}
	}
	ELSE
	{
	IF (the SnkNodeID equals 'this' node's ID, and the
	BroadcastID has not been previously processed)
	{
	Deliver Payload up the protocol stack;
	}
	}

Table 10. CODEAN Message Processing

A simulation of an ad hoc network using the CODEAN routing protocol was developed using the C++ programming language. Figure 10 shows some examples of the results of the simulation of the CODEAN protocol for various cluster sizes. For the cluster size of $M = 1$, the result is a bucket brigade configuration similar to a conventional ad hoc network. Increasing the cluster size produces an approximate synthetic waveguide configuration. The first cluster of the waveguide is situated near the source nodes so that the source message is reliably transferred to every relay node within the first cluster. For a large cluster size (such as $M = 8$), the communication route is clearly asymmetric. If the 'sink' node (as marked in Figure 10) has information to send to 'source' node, simply reversing source-to-sink route would perform poorly because of the long first hop from the 'sink' node to the nearest cluster. Unlike most ad hoc networking protocols, the CODEAN protocol does not automatically create a sink-to-source route during the process of setting up the source-to-sink route. For the 'sink' node to send DATA packets to the 'source' node, the 'sink' node must establish a new route back to the source node via a ROUTE_REQUEST message.

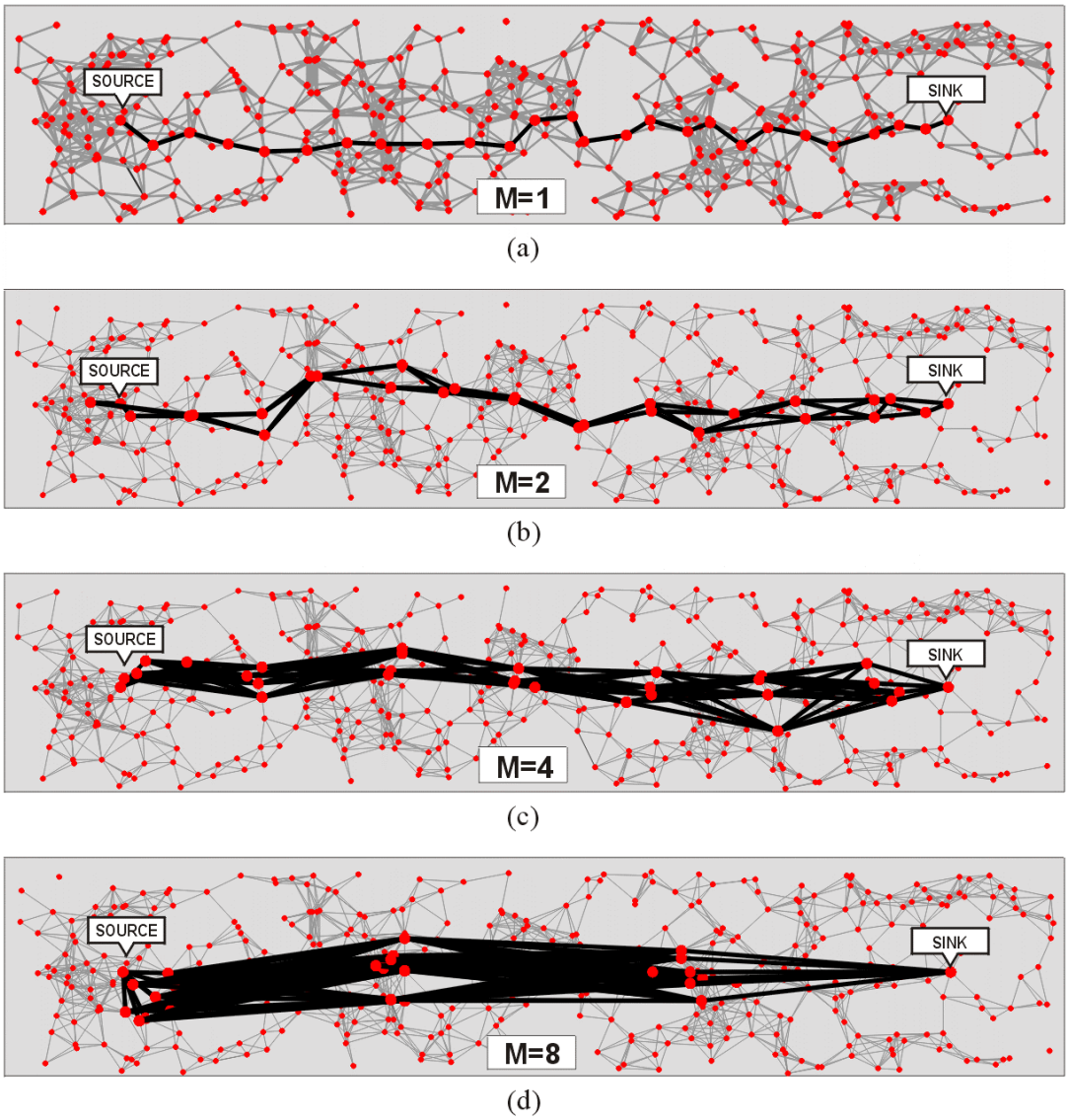

Figure 10. CODEAN Routing Examples

The CODEAN protocol creates an approximate synthetic waveguide among the randomly dispersed relay nodes. The next chapter describes the derivation of the information theoretic capacity of the synthetic waveguide.

III. CHANNEL CAPACITY OF THE SYNTHETIC WAVEGUIDE

The goal of this chapter is to develop the information theoretic channel capacity of the Synthetic Waveguide (SW) in a Nakagami-m faded, additive Gaussian noise environment. Two different modes of communication are examined. The first mode is called maximum redundancy, where the goal is that *every* node participating in the synthetic waveguide decodes a copy of the source message with an arbitrarily small number of errors. The second mode is called maximum rate, where the highest possible rate of data flow from the source node to the sink node is sought for which the decoded message at the sink node has an arbitrarily small number of errors. Before deriving the channel capacity, the next two sections define the synthetic waveguide channel and describe an upper bound on the maximum possible rate of information flow through the synthetic waveguide.

A. THE ENVIRONMENTAL MODEL

This section describes the environmental communication model used in the channel capacity analysis of the synthetic waveguide.

The key parameters defining the synthetic waveguide configuration and the fading channel environment are listed in Table 11. We assume that the signal power is attenuated according to a constant path loss exponent of $\alpha = 4$. The average received power at the antenna of a relay node in the adjacent cluster is a function of distance, which is defined as

$$\mathcal{E}_r(d) \triangleq \mathcal{E}_S \left(d/d_M\right)^{-\alpha} . \tag{2}$$

where $\mathcal{E}_S$ is the average transmitted signal power measured at some distance d_M that is outside of the near field of the transmit antenna. For the remainder of this thesis, assume that $d_M = 1$ and $\mathcal{E}_S$ is the average signal power at a unit distance from the transmitter for some omnidirectional antenna.

Let d_0 be the nominal distance between adjacent nodes for a cluster size of $M = 1$ (the bucket brigade); then, the average received power at each relay node is

$$\mathcal{E}_r = \mathcal{E}_S \left(M\, d_0\right)^{-\alpha} \tag{3}$$

Symbol	Description	Value
H	Number of Hops	—
M	Number of Relay Units per Cluster	1,2,4,8
d_0	Nominal Link Distance (for M = 1)	1
$\mathcal{E}_S$	Nominal Relay Transmit Power	—
N_0	Nominal Received Noise Power	—
α	Path Loss Exponent	4
m	Nakagami-m fading factor	0.1 – 3

Table 11. Synthetic Waveguide Parameters

The environmental communication model used for the analysis of the capacity of the synthetic waveguide is depicted in Figure 11. The energy of every transmitted signal is attenuated by both path loss and Nakagami-m fading. The relay units within a cluster transmit simultaneously, and the transmitted waveforms sum noncoherently on the receiving relay's antenna. The thermal noise (Gaussian) is added at every receiver. The path length between relays in adjacent clusters is assumed to be equal. All links between relays are independently and identically faded.

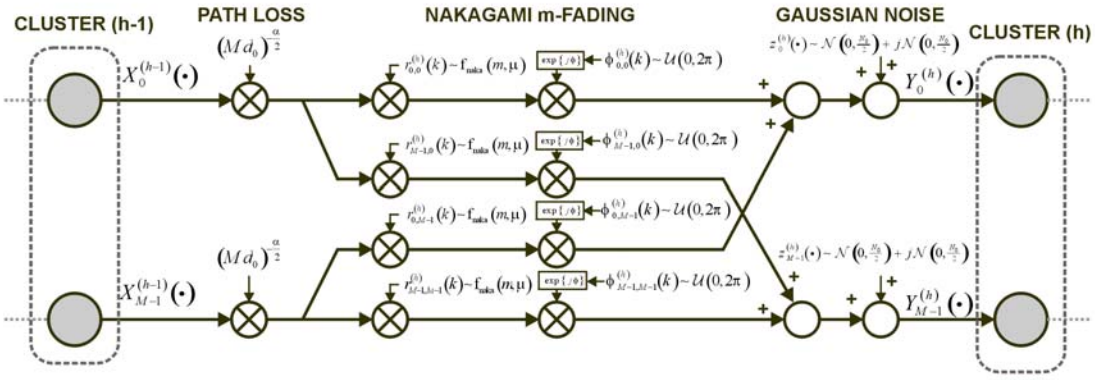

Figure 11. Environmental Communication Model

If the distance from one cluster to another is much greater than the distance between relay units within a cluster, then the fading among the various signal paths is likely to be correlated [1]. Such correlation is ignored and the fading statistic of every communication path is assumed to be independent of the fading statistic of every other communications path.

The transmitted signal waveform is assumed to consist of L-long blocks of symbols that comprise a given packet of data (any additional symbols necessary for

synchronization or other overhead functions are neglected in this analysis). We assume that the fading channel's coherence time exceeds the packet length such that all of the transmitted symbols in each packet are faded (attenuated and rotated) in an identical fashion.

Let $X_m^{(h)}(i+kL)$ represent the signal waveform transmitted from the m^{th} relay node within the h^{th} cluster of the synthetic waveguide. The received signal at a node within the next adjacent cluster is

$$Y_m^{(h)}(i+kL) = (M\,d_0)^{-\frac{\alpha}{2}} \sum_{m'=0}^{M-1} r_{m,m'}^{(h)}(k) \exp\left(j\,\phi_{m,m'}^{(h)}(k)\right) X_{m'}^{(h-1)}(i+kL) + Z_m^{(h)}(i+kL) \tag{4}$$

where

h is the cluster number within the synthetic waveguide,

m is the index of the relay node within the h^{th} packet,

k is the packet index number, and

i is the index of the symbol with in the k^{th} packet.

Each channel gain coefficient $r_{m,m'}^{(h)}(k)$ is modeled as a random variable that is independently and identically distributed according to the Nakagami-m fading envelope distribution with unit mean, or

$$r_{m1,m1'}^{(h1)}(k1) \sim \mathrm{f}_{\mathrm{naka\_m}}(m,\mu)\big|_{\mu=1}, \forall\{h1,,k1,,m1,m1'\} \tag{5}$$

and

$$r_{m1,m1'}^{(h1)}(k1) \perp r_{m2,m2'}^{(h2)}(k2), \forall\{h1,k1,m1,m1'\} \neq \{h2,k2,m2,m2'\} \tag{6}$$

where $\mathrm{f}_{\mathrm{naka\_m}}(m,\mu)$ is the Nakagami-m probability density function (pdf).

Similarly, each channel phase rotation coefficient $\phi_{m,m'}^{(h)}(k)$ is modeled as a random variable that is independently and identically distributed according to a uniform distribution ranging over the interval $[0,2\pi)$, or

$$\phi_{m,m'}^{(h)}(k) \sim \mathcal{U}(0,2\pi), \forall\, h,k,\, m,m' \tag{7}$$

and

$$\phi_{m1,m1'}^{(h1)}(k1) \perp \phi_{m2,m2'}^{(h2)}(k2), \forall\{h1,,k1,,m1,m1'\} \neq \{h2,k2,m2,m2'\} \tag{8}$$

Finally, the additive thermal noise at the receiver of each relay node $z_m^{(h)}(i')$ is modeled as a random variable that is independently and identically distributed according to a complex Gaussian random variable with zero mean and a variance of N_0, or

$$Z_m^{(h)}(i') \sim \mathcal{N}\left(0, \tfrac{N_0}{2}\right) + j\,\mathcal{N}\left(0, \tfrac{N_0}{2}\right), \forall\, h,\, m, i' \tag{9}$$

and

$$Z_{m1}^{(h1)}(i1) \perp Z_{m2}^{(h2)}(i2), \forall \{h1, m1, i1\} \neq \{h2, m2, i2\} \quad . \tag{10}$$

Defining the fading channel coefficients as $g_{m,m'}^{(h)}(k)$, we get

$$g_{m,m'}^{(h)}(k) \triangleq r_{m,m'}^{(h)}(k) \exp\left(j\,\phi_{m,m'}^{(h)}(k)\right) \ . \tag{11}$$

The matrix for the channel gain between clusters is defined as

$$\underline{\underline{G}}^{(h)}(k) \triangleq \begin{bmatrix} g_{0,0}^{(h)}(k) & \cdots & g_{0,M-1}^{(h)}(k) \\ \vdots & \ddots & \vdots \\ g_{M-1,0}^{(h)}(k) & \cdots & g_{M-1,M-1}^{(h)}(k) \end{bmatrix} \tag{12}$$

and the channel may be expressed in matrix form as

$$\underline{Y}^{(h)}(i + LK) = (M\, d_0)^{-\frac{\alpha}{2}}\, \underline{\underline{G}}^{(h)}(k)\, \underline{X}^{(h-1)}(i + LK) + \underline{Z}^{(h)}(i + LK) \tag{13}$$

where the transmitted signal from each cluster of relay nodes is the vector

$$\underline{X}^{(h)}(i') \triangleq \left[X_0^{(h)}(i'), X_1^{(h)}(i'), \ldots, X_{M-1}^{(h)}(i') \right]^T \ . \tag{14}$$

The received signal vector at each cluster of relay nodes is

$$\underline{Y}^{(h)}(i') \triangleq \left[Y_0^{(h)}(i'), Y_1^{(h)}(i'), \ldots, Y_{M-1}^{(h)}(i') \right]^T \tag{15}$$

and

$$\underline{Z}^{(h)}(i') \triangleq \left[Z_0^{(h)}(i'), Z_1^{(h)}(i'), \ldots, Z_{M-1}^{(h)}(i') \right]^T \tag{16}$$

is the additive thermal noise at the receiver of each relay nodes in a given cluster.

A Nakagami-m faded signal envelope is distributed according to [1] as

$$\mathrm{f}_{\mathrm{naka\_m}}(r; m, \mu) \triangleq \frac{2 m^m r^{2m-1}}{\mu^m \Gamma(m)} \exp\left(-\frac{m r^2}{\mu}\right) \text{for } r \geq 0 \tag{17}$$

where m is the fading factor and μ is the average envelope amplitude.

The pdf for the Nakagami-m faded signal envelope with unit mean (see Figure 12) changes dramatically as a function of the fading factor. For, $m = 1$ the Nakagami-m fading pdf for the signal envelope is identical to the Rayleigh distribution. For $m > 1$, the Nakagami-m fading distribution becomes similar (but not identical) to the Ricean distribution and models the situation where the received signal contains a dominant

spectral component. As $m \to \infty$, the received signal possesses no fading variation. For $m < 1$, the distribution becomes heavily skewed towards zero implying frequent and deep fades.

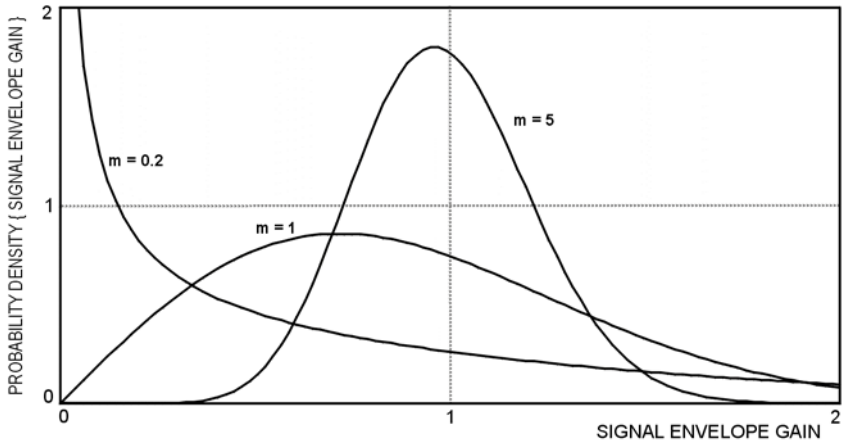

Figure 12. Nakagami-m Probability Density Function (Envelope)

The signal power is defined as

$$\mathcal{E} \triangleq r^2 \tag{18}$$

and making a change in the variable of the pdf, one finds

$$\mathrm{f}_{\mathrm{naka\_m}}(\mathcal{E}) = \frac{m^m \mathcal{E}^{m-1}}{\mu^m \Gamma(m)} \exp\left(-\frac{m\mathcal{E}}{\mu}\right) \text{for } \mathcal{E} \geq 0 \tag{19}$$

which is the pdf for a faded signal power level. This pdf is plotted for several values of m in Figure 13.

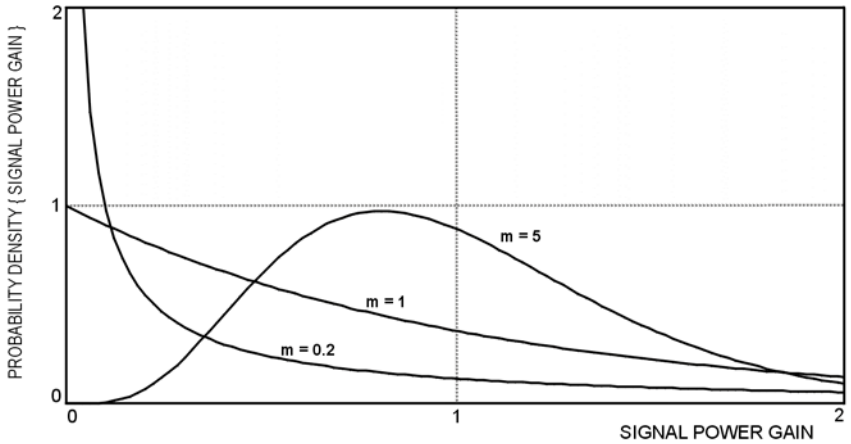

Figure 13. Nakagami-m Probability Density Function (Power)

To convert this signal power to decibels,

$$x_{dB} \triangleq 10\log(\varepsilon) \tag{20}$$

and again making a change in the variable of the pdf, one finds

$$\mathrm{f}_{\mathrm{naka\_m}}(x_{dB};m,\mu) = \frac{\ln(10)}{10}\frac{m^m\left(10^{\frac{x_{dB}}{10}}\right)^m}{\mu^m\Gamma(m)}\exp\left(-\frac{m}{\mu}10^{\frac{x_{dB}}{10}}\right) . \tag{21}$$

This pdf as a function of dB signal gain is plotted for several values of m in Figure 14. Another common fading distribution is the lognormal shadowing distribution. The pdf of the lognormal shadowing distribution as a function of dB signal gain is the Gaussian distribution with a zero mean. For $m >> 1$, the Nakagami-m fading pdf appears very similar to a Gaussian pdf; however for $m < 1$, the Nakagami-m fading model produces many more deep fades than the lognormal shadowing model.

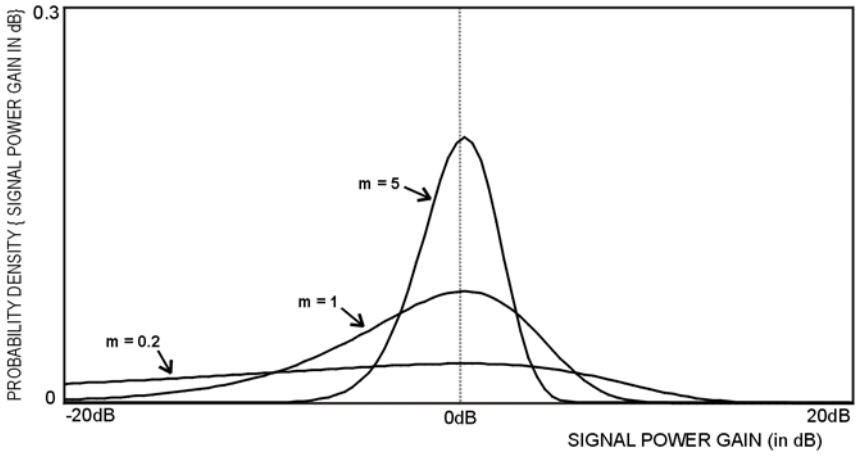

Figure 14. Nakagami-m fading Density (Signal Power Gain in dB)

B. AN UPPER BOUND ON THE CAPACITY OF THE SYNTHETIC WAVEGUIDE

In this section, an upper bound on the maximum capacity of the synthetic waveguide is derived.

Let X^N for$(X \in \mathcal{X})$ represent the N symbol message that the source node wishes to send to the sink node via the synthetic waveguide, and let Y^N for$(Y \in \mathcal{Y})$ represent the channel output received at the sink node.

The intervening relay nodes form a Markov chain as the information is passed from relay cluster to relay cluster.

Define

$$C^{(h)^N} \triangleq \left\{ X_o^{(h)}, X_1^{(h)}, \ldots, X_{M-1}^{(h)} \right\}^N \tag{22}$$

to represent all of the information received at the h^{th} cluster.

This analysis assumes that every receiving node in a given cluster has perfect information about the state of the channel including signal gain and rotation due to fading.

Let $S^{(h)}$ represent this channel state information; specifically,

$$S^{(h)} \triangleq \left\{ g_{m,m'}^{(h)}(k) \forall m, m', k \right\} \text{ for } h = 1, 2 \ldots H-1 \tag{23}$$

for the intermediate relay nodes, and let

$$S_Y \triangleq \left\{ g_{m,m'}^{(H-1)}(k) \forall m, m', k \right\} \tag{24}$$

for the final hop into the sink node.

Also, each node is aware of the static synthetic waveguide parameters listed in Table 11 (such as the average transmitted signal power and average thermal noise energy). In practice, the receiving nodes would have to estimate these parameters from the received signal; however, since these parameters change slowly (once per packet for the channel fading coefficients), each receiver has many channel observations to achieve an accurate estimate of the various unknown parameters.

The transfer of information from one cluster to the next is governed according to the conditional channel probability function

$$p\left(C^{(h)^N} \mid C^{(h-1)^N}, S^{(h)} \right). \tag{25}$$

Because the channel probability function is independent (given the channel state for each sequentially transmitted symbol), the conditional channel probability function may be factored as

$$p\left(C^{(h)^N} \mid C^{(h-1)^N}, S^{(h)} \right) = \prod_{n=0}^{N-1} p\left(C^{(h)^i} \mid C^{(h-1)^i}, S^{(h)} \right). \tag{26}$$

Therefore, given the channel state, the channel is said to be memoryless.

To simplify the problem in order to develop an upper bound on the channel capacity, suppose that the nodes within a given cluster may share any amount of information among one another. In the actual synthetic waveguide, each relay must operate autonomously and does not share information with other cluster members. However, the channel capacity of the synthetic waveguide cannot decrease if we allow the sharing of information among the nodes within a given cluster because

$$\begin{aligned} \mathrm{H}\left(C^{(h)^N} \mid C^{(h-1)^N}, S^{(h)} \right) &= \sum_{m=0}^{M-1} \mathrm{H}\left(X_m^{(h)^N} \mid \bigcup_{m'=0}^{m} X_{m'}^{(h)^N}, C^{(h-1)^N}, S^{(h)} \right) \\ &\leq \sum_{m=0}^{M-1} \mathrm{H}\left(X_m^{(h)^N} \mid C^{(h-1)^N}, S^{(h)} \right) \end{aligned} \tag{27}$$

The uncertainty about the transmitted message in an individual relay node given the information it received from the previous cluster is greater than the joint uncertainty about the transmitted message among all of the nodes within a cluster given the information the cluster of nodes received from the previous cluster. This is a consequence of the independence bound on entropy (see [13]), where H(X) is the Shannon entropy function, which is defined as

$$\mathrm{H}(X) \triangleq -\sum_{X \in \mathcal{X}} p(X) \log_2 \left(p(X) \right). \tag{28}$$

The source node encodes the information that it intends to share with the sink node into a block of N symbols. This information is passed from cluster to cluster forming a Markov chain (see Figure 15). The relay nodes within a cluster listen to the incoming message until the entire block of N symbols is received. This block is broken up into many L-symbol packets for transmission, so many different fading conditions are observed during the exchange of the source information.

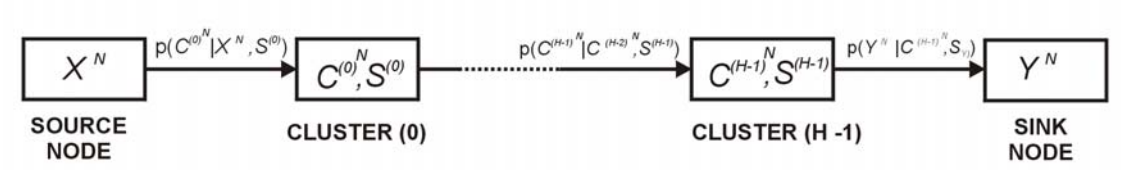

Figure 15. Synthetic Waveguide Markov Chain

To determine the capacity of the synthetic waveguide (cluster-to-cluster transfer), we wish to avoid complications arising from the termination of the synthetic waveguide at the source and sink node. Therefore, we assume that the source message is reliably passed from the source node into the first cluster and that the information about the source message known to the last cluster is reliably passed to the sink node.

The reliable transfer of the source node information into each of the nodes in the first cluster implies that

$$\mathrm{H}\left(X^N \mid C^{(0)^N}, S^{(0)} \right) = 0, \tag{29}$$

which states that given the information received at the first cluster, the uncertainty about the source message reduces to zero.

The assumption that information is reliably transferred from the last cluster into the sink node implies that

$$\mathrm{H}\left(C^{(H-1)^N}, S^{(H-1)} \mid Y^N, S_Y\right) = 0\,. \tag{30}$$

By this assumption, the sink node has access to the same information as the last cluster of relay nodes including knowledge of the channel state. Equivalently, one could imagine that the nodes within the last cluster send the sink node copies of the waveforms they each receive on their respective antennas, so that the sink node may extract the information held jointly by last cluster of relay nodes.

THEOREM 1: (Upper Bound on the Capacity of the Synthetic Waveguide)

Given the synthetic waveguide channel, if there exists a $(2^{R_{XY}N})$ block code containing $2^{R_{XY}N}$ possible codewords (or distinct messages) transmitted using a block of N symbols for which the number of received errors is arbitrarily low, then

$$R_{XY} \le \mathrm{E}_{fading}\left\{\log_2\left(\left|I_{MxM} + A_S\, M^{-\alpha}\, \underline{\underline{G}}\, \underline{\underline{G}}^{H}\right|\right)\right\} \tag{31}$$

where H is the Hermitian (the conjugate transpose operator on a matrix), R_{XY} is the code rate, $\underline{\underline{G}}$ is the matrix of channel fading coefficients (defined in Equation (12)), A_S is the normalized transmitted signal power defined as

$$A_S \triangleq \frac{\mathcal{E}_S}{N_0} d_0^{-\alpha}\,, \tag{32}$$

and the expectation is taken with respect to the channel coefficient fading distribution (see Equations (5), (7), and (17)).

PROOF:

Shannon's channel capacity theorem states that for memoryless channels, the code rate R_{XY} must be less than the maximum average mutual information shared by the source node and the sink node (see [13]), or

$$R_{X,Y} \le \max_{P(x)} \mathrm{I}\left(X;Y\right). \tag{33}$$

From the data processing inequality (see [13]), the average mutual information between the source and sink nodes must be greater than the average mutual information between any pair of clusters of relay nodes, or

$$R_{X,Y} \le \max_{P(x)} \mathrm{I}(X;Y) \le \min_{m=1,\ldots H-1} \max_{P(C^{(m)})} \mathrm{I}\left(C^{(h)};C^{(h-1)} \mid S^{(h)}\right). \tag{34}$$

Because the statistical channel description between every pair of adjacent clusters is identical, the channel capacity reduces to finding the maximum capacity between any pair of adjacent clusters,

$$R_{X,Y} \le \max_{P(C^{(h)})} \mathrm{I}\left(C^{(h)};C^{(h-1)} \mid S^{(h)}\right). \tag{35}$$

Because the nodes within each cluster are allowed to share information with each other, we may consider each cluster as an integrated unit possessing M transmit/receive antennas. So finding the upper bound on the capacity reduces to finding the capacity of the Multiple Input Multiple Output (MIMO) channel (see Figure 16).

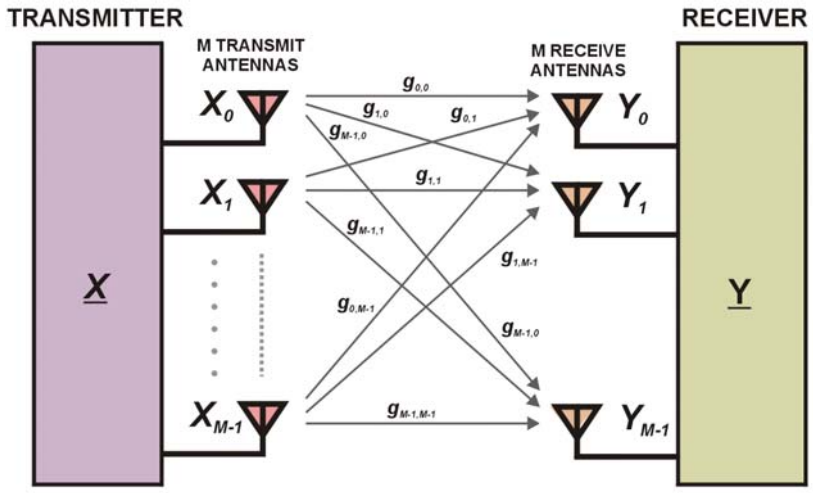

Figure 16. Multiple Input Multiple Output Channel

Recall that the coherence time of the channel is assumed to exceed the time required to transmit a single packet. For a given packet, the channel fading coefficients are fixed, and the channel between adjacent clusters becomes a simple multidimensional Gaussian channel. Provided that the number of symbols within the packet is large, then the capacity of this stationary MIMO Gaussian channel is well known to be (see [13] or [14])

$$C_{MIMO\_UNFADED} = \log_2\left(\left|I_{MxM} + A_S\, M^{-\alpha}\, \underline{\underline{G}}\,\underline{\underline{G}}^{H}\right|\right). \tag{36}$$

To achieve this capacity, the transmitted waveforms must be Gaussian distributed, and the relay nodes within the transmitting cluster need to know the channel coefficients in order to adjust their coding rate to less than the channel capacity for each packet [15].

In the definition of the synthetic waveguide, each relay node transmits using the same average power per packet, so regardless of the actual channel capacity for a given coherence time, relay nodes within the transmitting cluster cannot readjust their transmit power to optimize the throughput for each packet. Further, in [16], the Gaussian channel is shown to satisfy the compatibility constraint. This implies that a fixed codebook for Gaussian distributed transmitted waveforms can achieve capacity even when the transmit power may be changed on every packet transmission. Because average transmit power is the only parameter that every node in the transmitting cluster need adjust in order to optimize capacity for a specific set of channel fading coefficients and because such adjustments are denied in the definition of the synthetic waveguide, the channel capacity over the fading channel is simply the averaged channel capacity (see [16] for additional details), or

$$C_{MIMO} = \mathrm{E}_{fading}\left\{\log_2\left(\left|I_{MxM} + A_S\, M^{-\alpha}\, \underline{\underline{G}}\, \underline{\underline{G}}^{H}\right|\right)\right\} \tag{37}$$

where the expectation is taken with respect to the fading distribution. This capacity for the faded MIMO channel is an upper bound on the channel capacity of the synthetic waveguide.

QED

C. THE CAPACITY OF THE MAXIMUM REDUNDANCY MODE

For the maximum redundancy mode of operation, the message generated by the source node must be reliably distributed to every node participating in the synthetic waveguide as opposed to just the sink node. This mode of operation could be useful for a multicast-style protocol.

THEOREM 2: (Capacity of the Synthetic Waveguide in Maximum Redundancy Mode)

Given the synthetic waveguide channel, there exists a $(2^{R_{XY}N})$ block code containing $2^{R_{XY}N}$ possible codewords (or distinct messages) transmitted using a block of N symbols for which the number of received errors is arbitrarily low if

$$R_{XY} \le \mathrm{E}_{fading}\left\{\log_2\left(1 + A_S\, M^{-\alpha} \sum_{m=0}^{M-1} r_m^2\right)\right\}, \tag{38}$$

where R_{XY} is the code rate, r_m (for m=0,1,…,M-1) are the fading channel envelope coefficients (defined in Equation (5)), A_S is the normalized transmitted signal power defined as

$$A_S \triangleq \frac{\mathcal{E}_S}{N_0} d_0^{-\alpha}, \tag{39}$$

and the expectation is taken with respect to the channel fading distribution (see Equations (5) and (17)).

The normalized transmitted signal power A_S is the average signal-to-noise ratio at the receiving relay node for the bucket brigade configuration (where the cluster size is $M = 1$). Recall that the goal is to find the synthetic waveguide configuration that uses the least amount of transmit power to obtain a given amount of data throughout. The normalized transmitted signal power allows a fair comparison between various synthetic waveguide configurations because it is consistently proportional to the actual transmitted power of every relay node.

PROOF:

As before, because each hop is identical, the problem reduces to the exchange of information between adjacent clusters of relay nodes. Returning to the original concept of the synthetic waveguide, we see that each relay node within the cluster operates autonomously and does not exchange information with neighboring cluster members.

Assume that the source message in the form of a block of N symbols has been reliably communicated to every node within the $(h-1)^{th}$ cluster. The task is to now transfer this information into every node within the $(h)^{th}$ cluster (see Figure 17). Because the channel is symmetric, the situation is identical for every node in the $(h)^{th}$ cluster. The transfer of information from the autonomous nodes of the $(h-1)^{th}$ cluster to any single node in the $(h)^{th}$ cluster is easily recognized as the Multiple Access Channel (MAC) as defined in [13] (page 399) or [17].

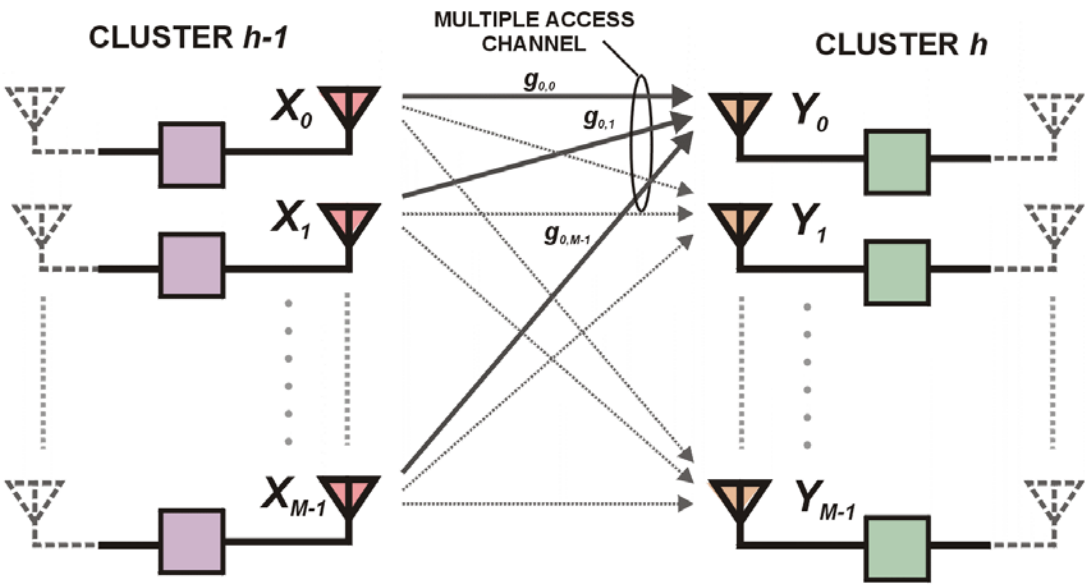

Figure 17. Multiple Access Channel

According to [13] (page 403), we have the capacity region of the *M*-user multiple access channel as

$$R(S) \le \mathrm{I}\left(X(S); Y \middle| X\left(S^{C}\right)\right) \forall\, S \subseteq \{0,1,\ldots,M-1\}. \tag{40}$$

This requires that the aggregate rate of any subset of nodes attempting to communicate with the receiver node must be less than or equal to the average mutual information between that set of nodes and the receiver node given the information within those nodes not within the subset.

The capacity of the multiple access channel is approached using Multi-User Detection (MUD) techniques, where M independent signals are transmitted into a single channel and arrive superimposed at the receiver. If the receiver can somehow demodulate $M-1$ of the signals error free, then receiver could re-modulate these $M-1$ signals and subtract them from the received waveform leaving just the single remaining un-demodulated signal in noise. In order to demodulate the remaining signal error free, the remaining signal must be above channel capacity. In order to demodulate all of the signals error free, all combinations of subsets of the signals must exceed channel capacity given those signals not in the given subset can be subtracted off at the receiver.

Because of symmetry (identical channel statistics) among every node within in the $(h)^{th}$ cluster and every node in the $(h-1)^{th}$ cluster, we let node 0 represent any given node within the $(h)^{th}$ cluster and the condition for an achievable code reduces to

$$m R_1 \le \mathrm{I}\left(\bigcup_{m'=0}^{m} X_{m'}^{(h-1)}; X_0^{(h)} \middle| \bigcup_{m'=m+1}^{M-1} X_{m'}^{(h-1)} \right) \forall\, m = 1, 2, \ldots, M \tag{41}$$

where R_1 is the information rate out of any node in the $(h-1)^{th}$ cluster.

Define

$$\underline{g}_n^{(h)}(m) \triangleq \left[g_{n,0}^{(h)}, g_{n,1}^{(h)}, \ldots, g_{n,m-1}^{(h)} \right] \tag{42}$$

as a set of m channel coefficients from the n^{th} row of the fading channel coefficient matrix defined in Equation (12).

As before, for a fixed set of channel coefficients, the capacity of the additive Gaussian channel is

$$\mathrm{I}\left(\bigcup_{m'=0}^{m-1} X_{m'}^{(h-1)}; X_0^{(h)} \middle| \bigcup_{m'=m}^{M-1} X_{m'}^{(h-1)} \right) = \log_2 \left(1 + A_s M^{-\alpha} \underline{g}_o^{(h)}(m) \underline{g}_o^{(h)H}(m) \right). \tag{43}$$

Also note that,

$$\underline{g}_o^{(h)}(m) \underline{g}_o^{(h)H}(m) = \sum_{m'=0}^{m-1} \left(r_{m',0}^{(h)} \right)^2; \tag{44}$$

therefore, an achievable code must satisfy each inequality within this set,

$$m R_1 \le \log_2 \left(1 + A_s M^{-\alpha} \sum_{m'=0}^{m-1} \left(r_{m',0}^{(h)} \right)^2 \right) \forall\, m = 1, 2, \ldots, M. \tag{45}$$

Because the channel with fixed fading coefficients is an additive Gaussian channel that satisfies the compatibility constraint described in [16] (also see the discussion in Theorem 1), the requirements for an achievable code for the fading channel are simply the inequality constraints of Equation (45) averaged over the channel fading distribution, or

$$m R_1 \le \mathrm{E}_{fading} \left\{ \log_2 \left(1 + A_s M^{-\alpha} \sum_{m'=0}^{m-1} \left(r_{m',0}^{(h)} \right)^2 \right) \right\} \forall\, m = 1, 2, \ldots, M. \tag{46}$$

This set of inequalities is dominated by the inequality when $m = M$ (see [13]). All hops within the synthetic waveguide have the same statistical description so the subscript identifying the specific hop and the specific node within a cluster may be removed. The requirement for an achievable code is thus

$$M R_1 \le \mathrm{E}_{fading} \left\{ \log_2 \left(1 + A_S M^{-\alpha} \sum_{m'=0}^{M-1} r_{m'}^2 \right) \right\} \tag{47}$$

and since R_1 is the code rate out of a single node, the total code rate for an achievable code is

$$R_{XY} = M\, R_1 \le \mathrm{E}_{fading}\left\{\log_2\left(1 + A_S\, M^{-\alpha} \sum_{m'=0}^{M-1} r_{m'}^2\right)\right\}. \tag{48}$$

QED

For the Nakagami-m fading channel, it is difficult to directly evaluate the expression for the channel capacity of the synthetic waveguide in the maximum redundancy mode from Equation (38). Therefore, an estimate of the channel capacity under various fading conditions was produced using Monte Carlo generation of 10,000 matrices of fading channel coefficients.

The channel capacity of the synthetic waveguide operating in maximum redundancy mode for a Nakagami-m fading factor of $m = 0.1$ is shown in Figure 18. The channel capacity for synthetic waveguide with cluster size ranging from one to four is nearly identical for the evaluated range of normalized transmitted signal powers. For a small normalized transmitted signal power level, the bucket brigade configuration has the highest channel capacity; but at large normalized signal power levels, the synthetic waveguide with a cluster size of two has a slight advantage in channel capacity. Increasing the cluster size to $M = 4$ does not improve performance.

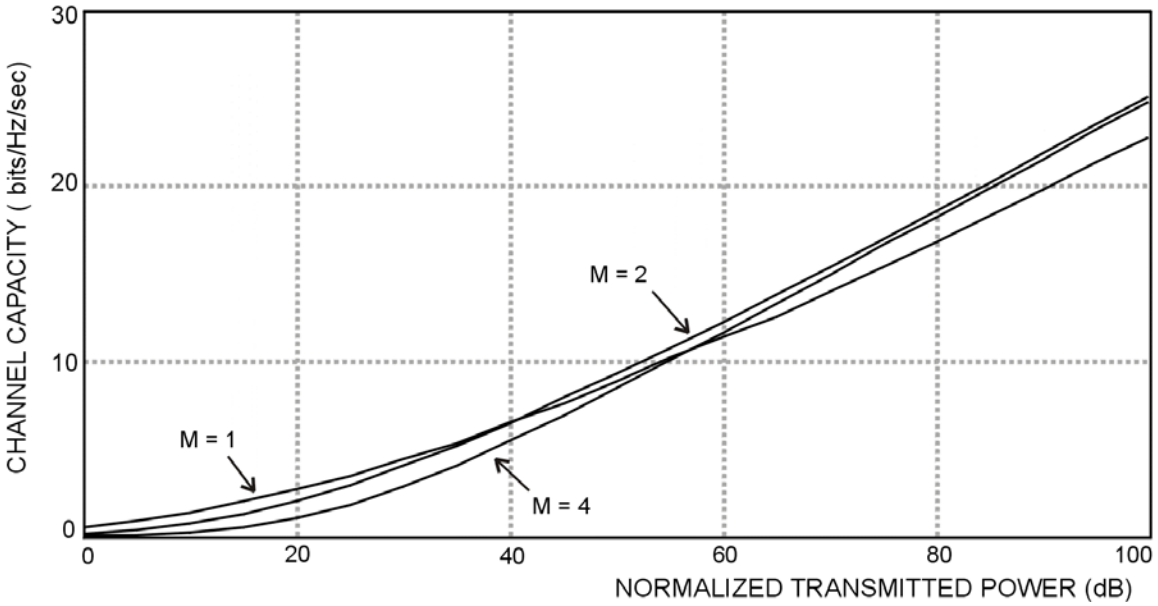

Figure 18. Maximum Redundancy Synthetic Waveguide Capacity for $m = 0.1$

In Figure 19, the normalized transmitted signal power is held fixed at 100 dB (a very high value), while the Nakagami-m fading factor is varied from 0.1 to 1. For moderate amounts of fading ($m = 1$, which is identical to Rayleigh fading), the traditional bucket brigade configuration is best. Only for a channel with extremely severe channel fading ($m < 0.2$) does increasing the cluster size of the synthetic waveguide appear to provide a potential improvement.

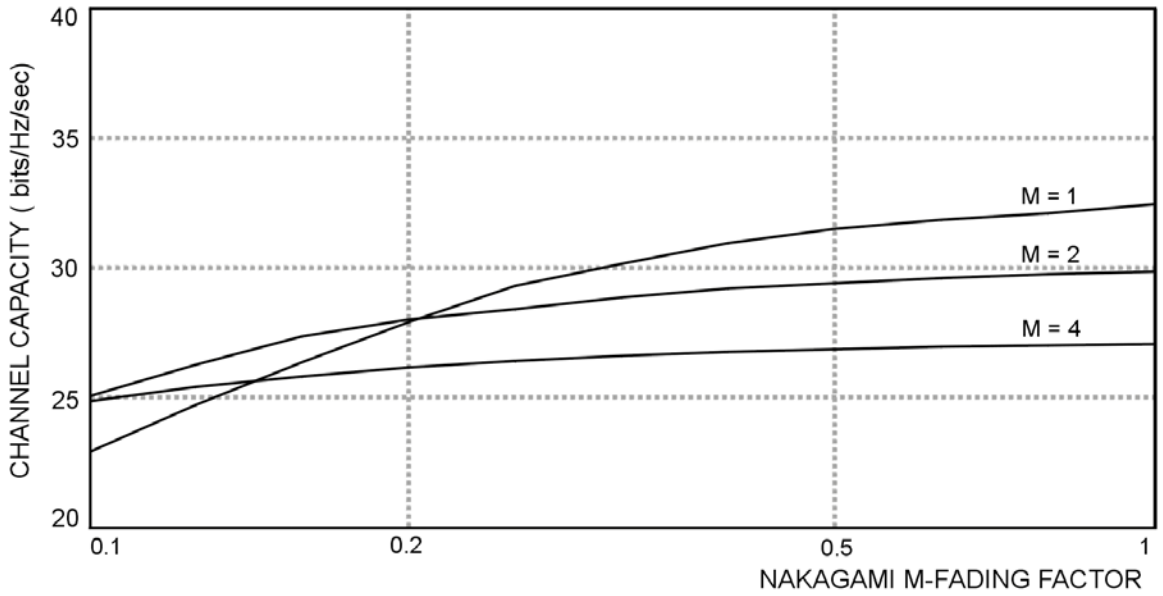

Figure 19. Maximum Redundancy Synthetic Waveguide Capacity for A_s = 100 dB

For any reasonable transmitted signal power level and/or for all but the most severely faded channels, the bucket brigade configuration, which is the methodology used in current ad hoc networks, provides the highest channel capacity.

Cooperative diversity and the synthetic waveguide methodology do not appear beneficial given the channel capacity results of the maximum redundancy mode of operation. However, the channel capacity results do favor cooperative diversity for the maximum rate mode, which is derived in the next section.

D. THE CAPACITY FOR THE MAXIMUM RATE MODE

For the maximum rate mode of operation, the message generated by the source node is intended only for the sink node. Whether or not any nodes along the synthetic waveguide can recover the message is unimportant. This mode of operation is useful to support a unicast style protocol.

THEOREM 3: (Capacity of the Synthetic Waveguide in Maximum Rate Mode)

Given the synthetic waveguide channel, there exists a $(2^{R_{XY}N})$ block code containing $2^{R_{XY}N}$ possible codewords (or distinct messages) transmitted using a block of N symbols for which the number of received errors is arbitrarily low if

$$R_{XY} \leq \mathrm{E}_{fading}\left\{\log_2\left(\left|I_{MxM} + A_S M^{-\alpha} \underline{\underline{G}}\,\underline{\underline{G}}^{H}\right|\right)\right\}, \tag{49}$$

where R_{XY} is the code rate, $\underline{\underline{G}}$ is the matrix of channel fading coefficients (defined in Equation (12)), A_S is the normalized transmitted signal power, which is defined as

$$A_S \triangleq \frac{\mathcal{E}_S}{N_0} d_0^{-\alpha}, \tag{50}$$

and the expectation is taken with respect to the channel fading distribution (see Equations (5), (7), and (17)).

PROOF:

The maximum channel capacity through the synthetic waveguide is limited by both the transfer of information into the sink node and by the intermediate hops through the synthetic waveguide. Again, each relay node within the cluster operates autonomously and does not exchange information with neighboring cluster members.

First, assume that the information from the source node has propagated error free to the next-to-last cluster (cluster $(h-1)$ in Figure 20). Recall that each relay node in the last cluster effectively passes its observation into the sink node (see Equation (30)) for joint processing; therefore, the relay nodes in the last cluster (and last cluster only) effectively share information among one another. So, the hop into the last cluster is a multiple access channel where M autonomous users (the relay node of cluster $(h-1)$) attempt to simultaneously pass as much information as possible into the last cluster. Because the relay nodes within the last cluster exchange information, the last cluster is viewed as a single processing unit with M antennas. This last hop is similar to the MIMO channel except that each transmitting relay node potentially has a different message to send.

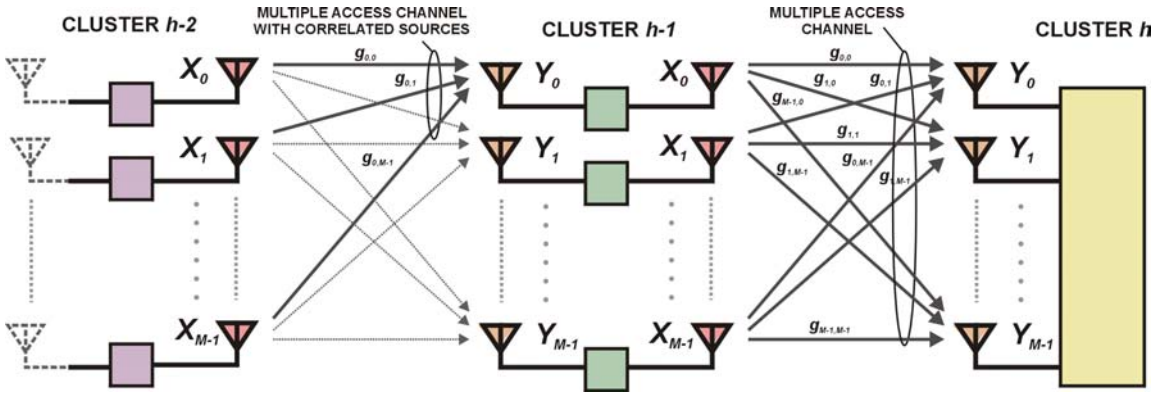

Figure 20. Cooperative Diversity / Synthetic Waveguide Channel

For the MIMO channel, the M antenna transmitter has access to the entire message to be sent, so that transmitted waveforms can be coordinated using space-time codes such as those described in [18] and [19]. For a MIMO multiple access channel, which is equivalent to the last hop of the synthetic waveguide, such codes cannot be used. However, the overall channel capacity is still identical to that of the MIMO channel (as shown below).

Again as in the proof of Theorem 2, the capacity region of the M-user multiple access channel is (see to [13]),

$$R(S) \le \mathrm{I}\left(X(S); Y \middle| X\left(S^C\right)\right) \forall\, S \subseteq \{0,1,\ldots,M-1\} \tag{51}$$

Again because of symmetry among every node in a given cluster, these inequality conditions for an achievable code reduce to

$$m\,R_1 \le \mathrm{I}\left(\bigcup_{m'=0}^{m} X_{m'}^{(h-1)}; \underline{X}^{(h)} \middle| \bigcup_{m'=m+1}^{M-1} X_{m'}^{(h-1)}\right) \forall\, m = 1,2,\ldots,M \tag{52}$$

where R_1 is the information rate out of any node in the $(h-1)^{th}$ cluster.

As in Theorem 2, for an additive Gaussian channel with fixed fading coefficients, this set of inequalities is dominated by

$$M\,R_1 \le \mathrm{I}\left(\bigcup_{m'=0}^{M} X_{m'}^{(h-1)}; \underline{X}^{(h)}\right) = \mathrm{I}\left(\underline{X}^{(h-1)}; \underline{X}^{(h)}\right) \tag{53}$$

where R_1 is the information rate out of any node in the $(h-1)^{th}$ cluster.

For a fixed set of fading channel coefficients, the average mutual information expressed in Equation (53) is

$$\mathrm{I}\left(\underline{X}^{(h-1)}; \underline{X}^{(h)}\right) = \log_2\left(\left|I_{MxM} + A_S\, M^{-\alpha}\, \underline{\underline{G}}\, \underline{\underline{G}}^{H}\right|\right). \tag{54}$$

As in Theorem 2, the channel with fixed fading coefficients is an additive Gaussian channel which satisfies the compatibility constraint described in [16]. The requirements for an achievable code for the fading channel are simply the inequality constraints of Equation (54) averaged over the channel fading distribution, or

$$M\,R_1 \le \mathrm{E}_{fading}\left\{\log_2\left(\left|I_{MxM} + A_S\,M^{-\alpha}\underline{\underline{G}}\,\underline{\underline{G}}^{H}\right|\right)\right\}. \tag{55}$$

Since R_1 is the code rate out of a single node, the total code rate is achievable code is

$$R_{XY} \le \mathrm{E}_{fading}\left\{\log_2\left(\left|I_{MxM} + A_S\,M^{-\alpha}\underline{\underline{G}}\,\underline{\underline{G}}^{H}\right|\right)\right\}. \tag{56}$$

This expression is identical to the channel capacity of the MIMO channel in a fading environment (see [14]). An achievable code exists for all code rates meeting the inequality in Equation (46), which is constrained by the upper bound from Theorem 1. Therefore, Equation (56) limits the maximum rate of information transfer into the last cluster.

Now, consider the hop from the $(h-2)^{th}$ cluster to the $(h-1)^{th}$ cluster. The situation appears very similar to the maximum redundancy mode analysis from the previous Chapter, where the relay nodes from the $(h-2)^{th}$ cluster attempt to communicate as much information as possible into a node within the $(h-1)^{th}$ cluster. Obviously, the capacity described in Equation (56) exceeds the expression for the capacity of the maximum redundancy mode of communication (see Equation (38)). This implies that to achieve any rate above the maximum redundancy mode, the channel capacity to some individual relay node shall be exceeded. However, the notion of operating above the individual channel capacity of a given receiver, while it is uncommon, is not as devastating as it seems.

Consider a highly simplified version of the synthetic waveguide channel shown in Figure 21. While this channel is noise and fading free, the same situation exists. Suppose that the signal waveform is restricted to Bi-Phase Shift Keying (BPSK), so that each transmitter is restricted to choose from $X \in \{+1,-1\}$. As shown in Figure 21, the received waveform is Y where $Y \in \{-2,0,+2\}$. Obviously, cluster 1 can only send 2 bits of information per channel to cluster 2 (because of the restricted signal set). When cluster 2 receives the pair $(Y_0^{(2)}, Y_1^{(2)})$, it can easily recover the original transmitted bits by calculating

$$\left(\widehat{X}_0^{(1)} = \frac{Y_0^{(2)} - Y_1^{(2)}}{2}, \widehat{X}_1^{(1)} = \frac{Y_0^{(2)} + Y_1^{(2)}}{2}\right). \tag{57}$$

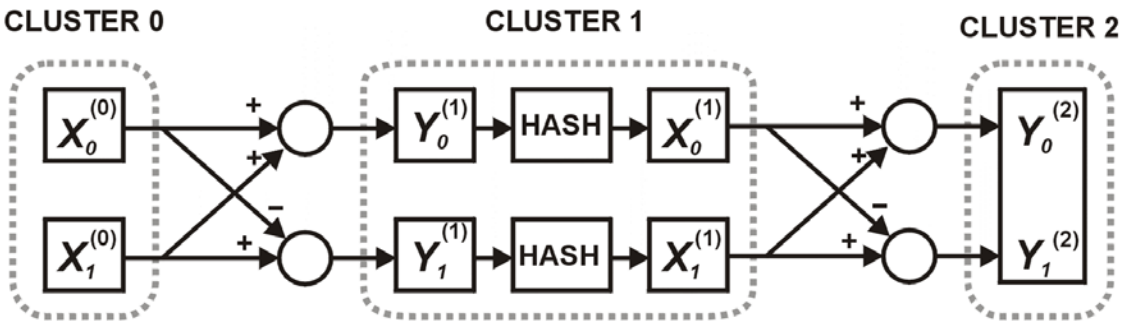

Figure 21. Noiseless Synthetic Waveguide Channel

Because cluster 2 has access to both observations ($Y_0^{(2)}, Y_1^{(2)}$), it can use joint processing to recover the transmitted data error free at the highest possible transmit capacity. This result illustrates what was just proven above for the last hop of the synthetic waveguide.

Now consider backing up to the hop from cluster 0 to cluster 1 (see Figure 21). The relay nodes within cluster 1 do not share information, so node 0 of cluster 1 only observes ($Y_0^{(1)}$) and from this observation, node 0 cannot determine either bit sent by the nodes in cluster 0. The entropy of ($Y_0^{(1)}$) is 1.5 (bits/channel use). If node 0 of cluster 1 could relay these 1.5 bits to cluster 2 while node 1 of cluster 1 sent its 1.5 bits of observation information, then cluster 2 could easily reconstruct the information sent by cluster 0.

The problem is that node 0 and node 1 of cluster 1 can each only send 1 bit of information, but each node of cluster 1 has 1.5 bits of uncertainty.

One option is for node 0 of cluster 1 to hash the 1.5 bits of uncertainty back into 1 bit of information and send that single bit of information to cluster 2. Node 1 of cluster 1 also defines a hash table. The result is depicted in Figure 22. For each observation, each node 1 must assign one bit value to send to cluster 2. Assume that these hash tables were shared with cluster 2 prior to this transmission. No matter how the assignment is made, this process introduces errors.

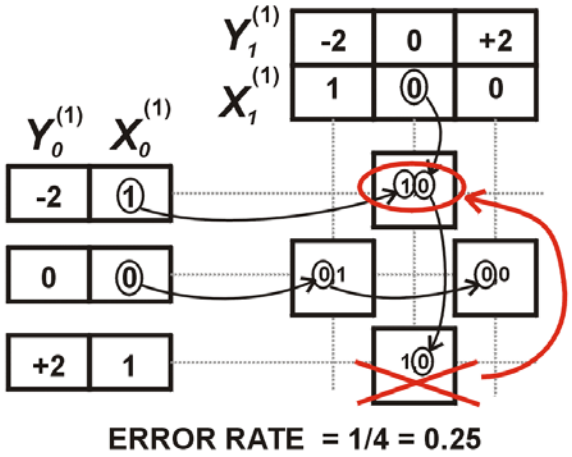

Figure 22. Compression Code for a Single Output Symbol

Consider what happens when the block length is increased from one symbol to two symbols as depicted in Figure 23. Each node in cluster 1 maps two observations symbols (with a total entropy of 3 (bits/channel use)) back into 2 bits. A hash map for the longer block length may be constructed to produce fewer errors. In fact, by increasing the block length, the error rate can be made arbitrarily small.

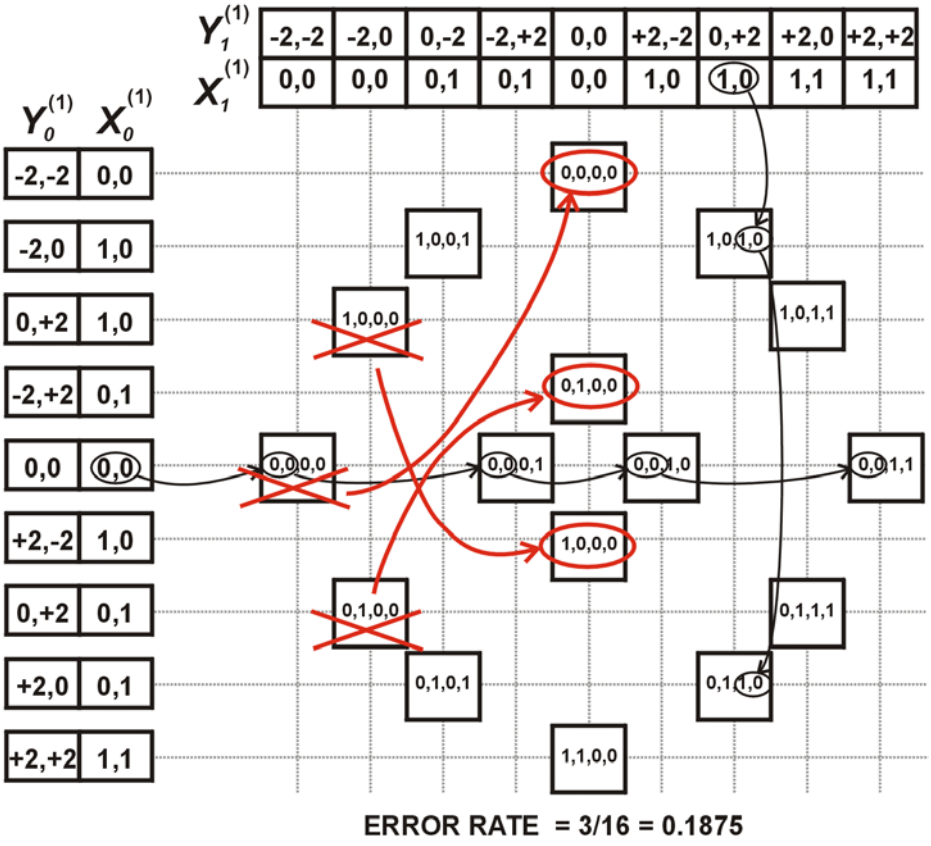

Figure 23. Compression Code for a Block of Two Output Symbols

This is the consequence of the Slepian and Wolf Data Compression Theorem for arbitrarily correlated sources [20]. While the sum of the entropy rate for each individual node in cluster 1 exceeds the channel capacity into cluster 2, an achievable compression scheme exists provided that the joint entropy among the nodes in cluster 1 is below the channel capacity into cluster 2.

The nodes in cluster 0 sent two bits of information, but only 1.5 bits were recovered in node 0 of cluster 1 because the nodes in cluster 0 sent information at a rate that exceeded that capacity of the channel into node 0 of cluster 1. Node 0 on cluster 1 has 0.5 bits of uncertainty per channel use. If one asked node 0 in cluster 1 what bits cluster 0 sent, node 0 of cluster 1 cannot arrive at an error-free answer; however, the uncertainty about the 2 bit message set by cluster 0 is reduced by 1.5 bits given the observation. Because the joint uncertainty of node 0 and node 1 of cluster 1 is below the channel capacity to cluster 2, then a distributed source compression code exists (given a long enough block length) with an arbitrarily low error rate.

This distributed source compression process (hashing) can be repeated for each cluster of relay nodes backing up to the first cluster, which has the source information. When the sink node receives its block of channel observations, it uses joint processing to determine the hashed index sent by the nodes in the previous cluster. Then a hash table search is performed to discover the hashed index sent by the nodes in the cluster one hop earlier. The sink repeatedly performs hash table lookups, each time discovering what the cluster next closer to source node knew. Finally, the last hash table lookup would reveal the source message. In practice, this repeated hash table lookup operation would likely produce errors unless the block length was impracticably long.

Relate this simple example back to the synthetic waveguide in a fading channel. Assume that every relay node within the $(h-2)^{th}$ cluster has an error-free copy of the source message. If the code rate of that message is above the channel capacity for the maximum redundancy mode, then the nodes within the $(h-1)^{th}$ cluster cannot decode the message in an error-free manner. Instead each node within the $(h-1)^{th}$ cluster will only be able to determine a set of messages for which the source message is a member. The size of this set of possible messages is $2^{N R_{EXCESS}}$ where N is the number of messages that the source node could choose from, and

$$R_{EXCESS} = \mathrm{E}_{fading}\left\{\log_2\left(\left|I_{MxM} + A_S\, M^{-\alpha}\, \underline{\underline{G}}\,\underline{\underline{G}}^{H}\right|\right) - \log_2\left(1 + A_S\, M^{-\alpha} \sum_{m'=0}^{M-1} \left|r_{m'}\right|^2\right)\right\}. \qquad (58)$$

So for every possible message transmitted by the $(h-2)^{th}$ cluster, each node within the $(h-1)^{th}$ cluster does not know which message was sent but, instead, each node has a set of possible messages that contains the message transmitted by the $(h-2)^{th}$ cluster. To pass the information forward to the last cluster of relay nodes, the relay nodes within the $(h-1)^{th}$ cluster cannot send the source message (because they do not know what it is). Instead a new and very large codebook is formed listing every possible set of messages, and then this large codebook is hashed into a codebook whose output can fit within the channel capacity to the $(h)^{th}$ cluster. The $(h)^{th}$ cluster can reconstruct the source message information by looking for the single message that is in common to all of the set of hashed indices reported by the relay nodes in the $(h-1)^{th}$ clusters.

The proof that this is possible is given by a modification to the Slepian and Wolf Data Compression Theorem by Cover, El Gamal, and Salehi for multiple access channels with arbitrarily correlated sources (see [20] or [17]). The channel capacity rates region for a distributed source coding of *M*-users with correlated sources that have no common information is given by

$$\mathrm{H}\left(U\left(S\right)|U\left(S^{C}\right)\right)\leq \mathrm{I}\left(X\left(S\right);Y|X\left(S^{C}\right),U\left(S^{C}\right)\right)\forall\, S\subseteq\{0,1,\ldots,M-1\} \tag{59}$$

where $U\left(S\right)$ represents the received information at a node before it is compressed into the transmitted codeword, $X\left(S\right)$.

Two random variables are said to contain common information if there exist a mapping from each random variable into a set such that any instance of these random variables map to the same member within this set with a probability of one (see [21]). The additive Gaussian noise element in the description of the synthetic waveguide prevents the occurrence of common randomness in this situation.

The inequality may be weakened by removing the conditioning on the right hand side of Equation (59), or

$$\mathrm{H}\left(U\left(S\right)|U\left(S^{C}\right)\right)\leq \mathrm{I}\left(X\left(S\right);Y|X\left(S^{C}\right)\right)\forall\, S\subseteq\{0,1,\ldots,M-1\}\,. \tag{60}$$

Because of symmetry among the statistical channel description of every node within the $(h-1)^{th}$ and $(h-2)^{th}$ cluster, the channel capacity rate region defined in Equation (60) becomes

$$\mathrm{H}\left(\bigcup_{m'=0}^{m}U_{m'}^{(h-2)}\middle|\bigcup_{m'=m+1}^{M-1}U_{m'}^{(h-2)}\right)\leq \mathrm{I}\left(\bigcup_{m'=0}^{m}X_{m'}^{(h-2)};\underline{X}^{(h-1)}\middle|\bigcup_{m'=m+1}^{M-1}X_{m'}^{(h-2)}\right)\forall\, m=1,2,\ldots,M\,. \tag{61}$$

The left hand side of Equation (61) describes the amount of joint uncertainty within a subset containing m nodes of the $(h-2)^{th}$ cluster. Assume that code rate of the cluster of nodes supplying information to the nodes of the $(h-2)^{th}$ cluster is under the channel capacity upper bound from Theorem 1.

Since the channel described is statistically identical for every hop, remove the hop index, and define a submatrix of the channel fading gain between clusters as (see Equation (12))

$$\underline{\underline{G}}_{m,n} \triangleq \begin{bmatrix} g_{0,0} & \cdots & g_{0,n-1} \\ \vdots & \ddots & \vdots \\ g_{m-1,0}(k) & \cdots & g_{m-1,n-1} \end{bmatrix}. \tag{62}$$

Then for the fading channel, the amount of joint uncertainty within a subset containing m nodes of the $(h-2)^{th}$ cluster is

$$\mathrm{H}\left(\bigcup_{m'=0}^{m} U_{m'}^{(h-2)} \middle| \bigcup_{m'=m+1}^{M-1} U_{m'}^{(h-2)} \right) = \mathrm{E}_{fading} \left\{ \log_2 \left(\left| I_{MxM} + A_S M^{-\alpha} \underline{\underline{G}}_{m,M-1} \underline{\underline{G}}_{m,M-1}{}^{H} \right| \right) \right\}, \tag{63}$$

and the average mutual information between this same set of m nodes of the $(h-2)^{th}$ cluster and the $(h-1)^{th}$ cluster is

$$\mathrm{I}\left(\bigcup_{m'=0}^{m2} X_{m'}^{(h-2)}; \underline{X}^{(h-1)} \middle| \bigcup_{m'=m2+1}^{M-1} X_{m'}^{(h-2)} \right) = \mathrm{E}_{fading} \left\{ \log_2 \left(\left| I_{mxm} + A_S M^{-\alpha} \underline{\underline{G}}_{M-1,m} \underline{\underline{G}}_{M-1,m}{}^{H} \right| \right) \right\}. \tag{64}$$

Recall the matrix identity for determinants

$$\left| I_{nxn} + \alpha A_{nxm} A_{nxm}{}^{H} \right| = \left| I_{mxm} + \alpha A_{nxm}{}^{H} A_{nxm} \right| \tag{65}$$

where A_{nxm} is a n by m complex valued matrix and α is any real-valued scalar.

Because each channel fading coefficient is independently and identically distributed within the matrix $\underline{\underline{G}}$, determinants in Equations (63) and (64) are equal,

$$\mathrm{E}_{fading} \left\{ \left| I_{MxM} + A_S M^{-\alpha} \underline{\underline{G}}_{m,M-1} \underline{\underline{G}}_{m,M-1}{}^{H} \right| \right\} = \mathrm{E}_{fading} \left\{ \left| I_{mxm} + A_S M^{-\alpha} \underline{\underline{G}}_{M-1,m} \underline{\underline{G}}_{M-1,m}{}^{H} \right| \right\}. \tag{66}$$

Therefore, the synthetic waveguide operates within the channel capacity rate region required by Equation (59) in order that a distributed source compression code exists allowing an arbitrarily low error rate.

For the Nakagami-m fading channel, direct numerical evaluation of the expression for the channel capacity of the synthetic waveguide in the maximum rate mode from Equation (49) is difficult. Consequently Monte Carlo approximation

averaging 10,000 matrices of fading channel coefficients were used to produce an estimate of the channel capacity under various fading conditions.

The channel capacity of the synthetic waveguide operating in the maximum rate mode for a severely faded channel with a Nakagami-m fading factor of $m = 0.1$ is shown in Figure 24. For large normalized transmitted signal power, the slope of the channel capacity for synthetic waveguide appears to become asymptotically proportional to the cluster size. This is similar to the MIMO channel in which capacity is proportional to the number of transmit and receive antennas.

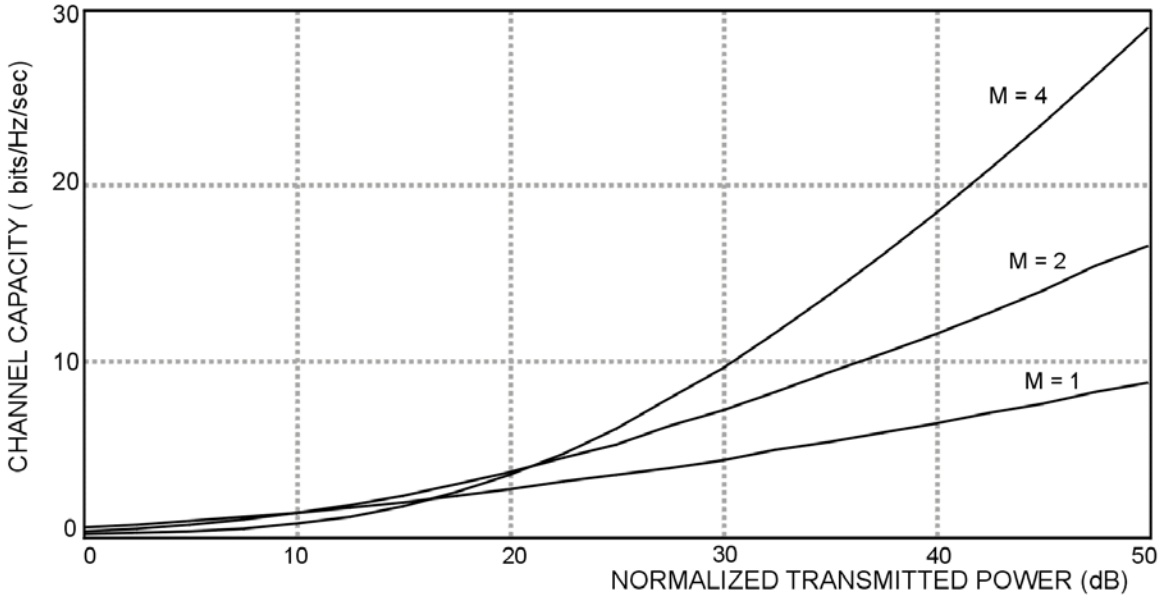

Figure 24. Maximum Rate Synthetic Waveguide Capacity for $m = 0.1$

The channel capacity of the synthetic waveguide operating in the maximum rate mode for a Nakagami-m fading factor of $m = 10$ is shown in Figure 25. This large Nakagami-m fading factor corresponds to a mild fading channel. The best channel capacity switches among synthetic waveguide configurations as a function of normalized transmitted signal power. For a small transmitted signal power, the bucket brigade $M = 1$ is best, but as the transmit power increases, the synthetic waveguide configuration with two nodes per clusters is optimal. At yet higher transmit power level, the synthetic waveguide configuration with four nodes power clusters is best (among the configurations shown). This behavior is expected because increasing the cluster size increases the distance to the adjacent cluster. With a path loss exponent of four, the increased distance dramatically reduces the received power at each node. In order to overcome this path loss, more transmit power is required. Given sufficient power, the

spatial diversity for a larger cluster size resists fading and opens parallel spatial communication channels supporting the increased slope with respect to the normalized transmitted power.

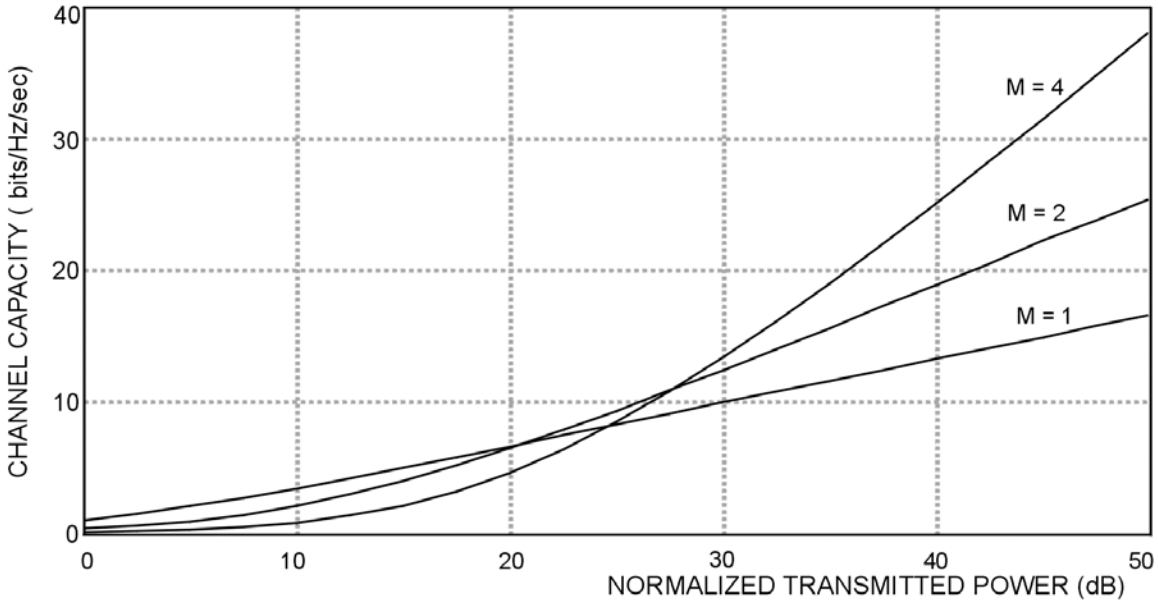

Figure 25. Maximum Rate Synthetic Waveguide Capacity for m =10

To achieve the channel capacity for either the maximum redundancy mode or the maximum rate mode requires that the block length of the overall message set by the source node greatly exceed the channel coherence time. Recall that the source message is broken up into many packets. Also, note that each relay node must observe the entire message before relaying any information to the next cluster. This allows the information in the message to be redundantly spread across many sets of fading channel conditions. This averaging prevents a single channel fade from inducing a deciding error, but the progress of the message through the synthetic waveguide is very slow.

For example, a typical channel coherence time may be 100 ms. Suppose that 100 packets are needed to send a message in order to allow for 100 different fading channel conditions. Each hop within the synthetic waveguide would take 10 s, and for many applications, this excessive latency would be unacceptable.

In the next Chapter, the capacity of the synthetic waveguide is developed for low latency transmission.

IV. LOW LATENCY CAPACITY OF THE SYNTHETIC WAVEGUIDE

The goal of this Chapter is to develop an information theoretic outage model based on the channel capacity of the Synthetic Waveguide (SW) in a Nakagami-m faded additive Gaussian noise environment under the additional restriction that the information transfer is low latency.

In the previous Chapter, the traditional channel capacity was derived for the synthetic waveguide. While traditional channel capacity reflects the absolute maximum rate of data flow, achieving this rate requires the entire block length (many data packets) to be received and processed at a given relay node before any information may be forwarded to the next relay node. This results in intolerably high latency as long blocks of data are buffered at each node along the communication path.

The definition of a low latency flow through the synthetic waveguide requires every relay node within a given cluster to retransmit a correctly received packet to the next adjacent cluster before the reception of the next incoming packet. Packets are assumed to contain an error detection mechanism (such as a Cyclic Redundancy Checksum (CRC)) and relay nodes only transmit whenever they have received the source message without error. Because decoding occurs on a packet-by-packet basis, the block length of the code used by the source node must be less than or equal to the length of a packet. This analysis is conducted using the maximum redundancy model, where ideally every relay node including the sink node will decode the source message with an arbitrarily small number of errors.

Three modes of modulation are studied. The first mode of modulation is called space-time coded modulation where each relay node within a cluster may transmit a different waveform to the adjacent cluster. The second mode of modulation is called simulcast modulation where each relay node within a cluster transmits the same identical waveform to the adjacent cluster. The third and final mode of modulation is called stuttered simulcast modulation where each relay node within a cluster generates the same waveform, but each node transmits this waveform to the adjacent cluster with an additional random phase modulation.

In this low latency mode of operation, not every relay node can possibly decode each packet error-free. Assume that k of M relay nodes within the $(h-1)^{th}$ cluster have received a packet of information error-free, and then these k of M relay nodes attempt to forward the source message to the relay nodes within the $(h)^{th}$ cluster. The operation is

similar to the multiple access channel analysis conducted in Chapter II, Section B; however, here only k of M nodes transmit instead of all M nodes.

Recall that for a fixed set of channel fading coefficients, the channel capacity of the additive Gaussian channel is

$$\mathrm{C}_{\mathrm{XY}}(k) = \log_2\left(1 + A_s M^{-\alpha} \underline{g}_o^{(h)}(k)\, \underline{g}_o^{(h)H}(k)\right) \tag{67}$$

where H is the Hermitian transpose and

$$\underline{g}_n^{(h)}(k) \triangleq \left[g_{n,0}^{(h)}, g_{n,1}^{(h)}, \ldots, g_{n,k-1}^{(h)}\right] \tag{68}$$

is the set of k channel coefficients from the n^{th} row of the fading channel coefficient matrix defined in Equation (12). The indices of the relay nodes within a cluster are reordered such that the k transmitting nodes are indexed for $m' = 0,1,\ldots k-1$. This reordering is possible because every relay node has the same statistical channel description.

The channel capacity is a function of the sum of the fading envelope coefficients,

$$\underline{g}_o^{(h)}(k)\, \underline{g}_o^{(h)H}(k) = \sum_{m'=0}^{k-1}\left(r_{m',0}^{(h)}\right)^2 \tag{69}$$

therefore, the code rate R_{XY} must satisfy

$$R_{XY} \le C_{XY}(k) = \log_2\left(1 + A_s M^{-\alpha} \sum_{m'=0}^{k-1}\left(r_{m',0}^{(h)}\right)^2\right) \tag{70}$$

to achieve an arbitrarily small number of errors (the packet length must also be sufficiently long).

The source node must choose a code rate for transmission without knowledge of the channel fading conditions. To ensure delivery of the packet with the desired reliability, the code rate must be below the capacity for the worst possible set of channel fading coefficients for which the probability of occurrence is on par with the overall desired error rate. This requirement quickly sends achievable code rates towards zero;

$$R_{XY} \le \min_{\underline{r} \sim \mathrm{f}_{\mathrm{naka\_m}}(\underline{r})} \log_2\left(1 + A_s M^{-\alpha} \sum_{m'=0}^{k-1}\left(r_{m',0}^{(h)}\right)^2\right) \to 0 \tag{71}$$

Instead, accept that within the context of the fading channel variations, sometimes the coding rate will be below the instantaneous channel capacity and then the packets shall decode with an arbitrarily small number of errors; however, whenever the coding

rate is above the instantaneous channel capacity, then the decoded packet shall contain errors.

The outage probability $P_{\bar{\gamma}}$ is the defined as the probability that a given packet will not decode with an arbitrarily small number of errors. Therefore,

$$P_{\bar{\gamma}} = \Pr\left\{ R_{XY} > C_{XY}(k) = \log_2\left(1 + A_s M^{-\alpha} \sum_{m'=0}^{k-1} \left(r_{m',0}^{(h)}\right)^2\right)\right\} \tag{72}$$

for a given set of fading channel envelope coefficients.

The remainder of this chapter assumes that an arbitrarily small number of errors is effectively equivalent to zero errors, such that the outage probability is the probability that a given packet will be decoded and detected (via the CRC) as error free.

All of the relay nodes within the first cluster are assumed to have an error-free copy of the source message; however as the message is propagated from cluster to cluster, localized channel fades may prevent some nodes from decoding the source message error-free.

The flow of communication from cluster to cluster along the synthetic waveguide with a cluster size $M = 8$ is depicted in Figure 26. As long as at least one relay node in a given cluster decodes the packets correctly, the information propagates forward. If no node within a given cluster decodes the information correctly, then the packet is lost and is not delivered to the sink node.

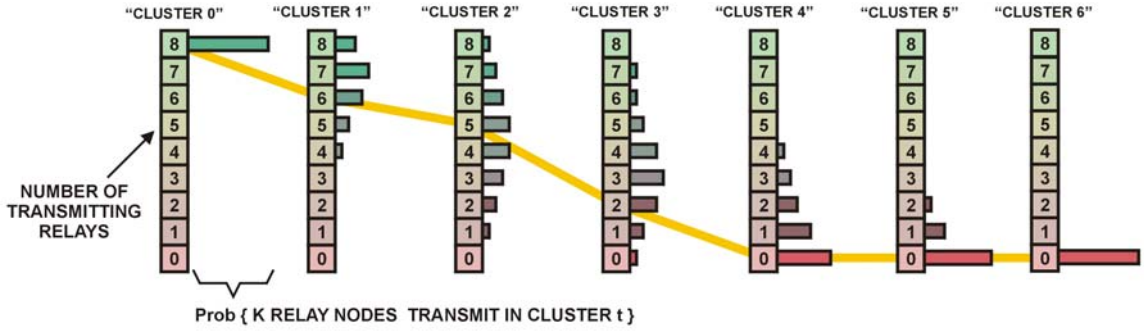

Figure 26. Synthetic Waveguide Markov Chain Model

Define a Markov chain to track the progress of information packets traversing the synthetic waveguide. The state vector of the Markov chain is a probability vector reflecting the number of relay nodes in the h^{th} cluster that have correctly received an error-free information packet. Relay nodes receiving an error-free information packet shall re-transmit that packet to relay nodes in the next forward cluster. The state probability vector is

$$\underline{q}^{(h)} \triangleq \begin{bmatrix} q_0^{(h)} & q_1^{(h)} & \cdots & q_M^{(h)} \end{bmatrix}^T \tag{73}$$

where

$$q_k^{(h)} \triangleq \Pr\{k \ \ relay \ \ nodes \ \ transmit \ \ at \ \ h^{th} \ \ hop\} \tag{74}$$

The transition matrix for the Markov chain is

$$Q_{j,k} \triangleq \Pr\{j \ \ relay \ \ nodes \ \ receive \mid k \ \ relay \ \ nodes \ \ transmit\} \tag{75}$$

$$= \binom{M}{j} \left(1 - P_{\bar{\gamma}|k,M}(A_s)\right)^j \left(P_{\bar{\gamma}|k,M}(A_s)\right)^{(M-j)} \tag{76}$$

where

$$P_{\bar{\gamma}|k,M}(A_s) \triangleq \Pr\{outage \mid k \ of \ M \ transmit \ using \ A_s\} \tag{77}$$

and $\binom{M}{j}$ is the number of combinations for choosing j of M items without replacement.

The state transition matrix Q advances the state vector q from the $(h-1)^{th}$ to the h^{th} hop by

$$\underline{q}^{(h)} = \underline{\underline{Q}} \ \ \underline{q}^{(h-1)}. \tag{78}$$

Assuming that the communication source is modeled as a cluster in which all relay units transmit or

$$\underline{q}^{(0)} = [\underbrace{0 \quad 0 \quad \cdots \quad 0}_{M-1} \quad 1]^T, \tag{79}$$

repeated application of Equation (78) yields the state probability vector for the h^{th} cluster

$$\underline{q}^{(h)} = \underline{\underline{Q}}^h \ \ \underline{q}^{(0)}. \tag{80}$$

The state transition matrix is structured as

$$\underline{\underline{Q}} \triangleq \left[\begin{array}{c|c} 1 & v_T \\ \hline 0 & \\ \vdots & Q_T \\ 0 & \end{array}\right]. \tag{81}$$

While only the q_0 state is recurrent (always returns to itself sometime in the future), all other states are transient. For every hop, each transient state has a non-zero probability that all forward relay units fail to receive the information packet error-free and that communication is lost (absorbed into the q_0 state).

Consider a probability state vector containing only the transient states of this Markov chain

$$\underline{q_T}^{(h)} \triangleq \begin{bmatrix} q_1^{(h)} & q_2^{(h)} & \cdots & q_M^{(h)} \end{bmatrix}^T. \tag{82}$$

This set of transient states form a class for which the probability of exiting this class is the same as the probability of a communication loss per hop or

$$q_0^{(h)} = \underline{v_T} \cdot \underline{q_T}^{(h-1)} \tag{83}$$

where $\underline{v_T}$ is the vector of probabilities that map the transient states into the recurrent loss state (see Equation (81)).

If the probability of loss is sufficiently small, these transient states become effectively recurrent among one another and yield a quasi-stationary limiting state probability vector (with a constant probability of exiting lost) as the number of hops reaches infinity.

$$(1-L)\underline{q_T}^{(\infty)} = \underline{\underline{Q_T}}\ \underline{q_T}^{(\infty)} \tag{84}$$

where

$$L = \Pr\left\{exiting\ \ per\ \ hop\right\} = \Pr\left\{communication\ \ loss\ \ per\ \ hop\right\}. \tag{85}$$

The Perron-Frobenius theory [22] allows us to determine L directly from the eigenanalysis of Q_T using

$$L = 1 - \lambda \tag{86}$$

where λ is the maximal eigenvalue of Q_T.

For a large number of hops, $\underline{q_T}^{(t)}$ should converge to its limiting probability vector, and the value of L represents the probability of communication loss per hop.

Given a synthetic waveguide with N relay nodes and a cluster size of M, the approximate number of hops required to traverse the entire link end-to-end is

$$\#\ \ hops \cong \frac{N}{M}\ \text{ for }\ N >> M\ . \tag{87}$$

Information packets successfully traverses the entire link with the probability

$$\Pr\left\{link\ \ closed\ \ end\ \ to\ \ end\right\} \cong (1-L)^{\frac{N}{M}}. \tag{88}$$

As N increases, so does the distance between the communication source and sink. To equitably compare different configurations, we wish to eliminate N by normalizing the probability of communication loss or outage per relay unit as

$$P_\ell \triangleq \Pr\left\{lost\ \ per\ \ relay\ \ unit\right\} = 1-(1-L)^{\frac{1}{M}}. \tag{89}$$

The outage per relay node probability may also be viewed as the complement of the geometric average of the probability of reception at any given relay unit. Given the

outage per relay node probability, the approximate probability that a packet shall be delivered to the sink node in a synthetic waveguide constructed on N relay nodes is

$$\Pr\{packet\ \ reaches\ \ sink\ \ node\} = 1-(1-P_\ell)^N . \tag{90}$$

The outage per relay node probability is evaluated and used to compare the performance of three different modulation modes in the next three sections.

A. SPACE-TIME CODED MODULATION MODE

The space-time coded mode of modulation is where each relay node within a cluster may transmit a different waveform to the adjacent cluster. Each relay node is aware of its uniquely assigned index within the cluster, which may be used to select the transmitted waveform. Each relay node is unaware of the number of nodes within its cluster that received the source message correctly.

In [23], Winters demonstrated a simple transmit diversity scheme in which the same waveform is delayed by a distinct number of symbols and each delayed version of the waveform is transmitted out of a separate antenna. The demodulator within the receiver uses a Maximum Likelihood Sequence Estimator (MLSE) to decode the received observation (after estimating the channel parameters). The performance of this modulation technique approaches the ideal Maximal Ratio Combiner (MRC).

This simple transmit diversity technique is also suitable for synthetic waveguide communication where the number of transmitting nodes is unknown. However, by correlating a known preamble sequence preceding each packet against the incoming waveform, the receiver could detect which delay offsets (among the set of possible delay offsets) were transmitted.

If the performance of the maximal ratio combiner is achieved, then the coding and demodulation scheme recovers an error-free packet whenever the coding rate is below the instantaneous channel capacity due to fading, and the probability of outage is

$$P_{\bar{\gamma}|k,M}(A_s) = \Pr\left\{R_{XY} > \log_2\left(1 + A_S\, M^{-\alpha} \sum_{m'=0}^{k-1} r_{m'}^2\right)\right\} \tag{91}$$

for k of M transmitting relay nodes. Rearranging, we get.

$$P_{\bar{\gamma}|k,M}(A_s) = \Pr\left\{\frac{2^{R_{XY}}-1}{A_s} M^{\alpha} > \sum_{m'=0}^{k-1} r_{m'}^2\right\} . \tag{92}$$

An outage occurs whenever the sum of the square of the Nakagami-m fading envelope coefficients is less than someconstant.If we define

$$\chi_k \triangleq \sum_{m'=0}^{k-1} r_{m'}^2 \text{ for } k = 1, 2\ldots, \tag{93}$$

then χ_1 is distributed according to Nakagami-m fading power distribution (with $\mu = 1$) defined in Equation (19). The characteristic function for this random variable is

$$\Phi_{\chi_1}(s) = \left(\frac{m}{m+s}\right)^m. \tag{94}$$

The characteristic function for the sum of k independent and identically distributed random variables is the product of their individual characteristic functions (see [24]) therefore,

$$\Phi_{\chi_k}(s) = \prod_{m'=0}^{k-1} \Phi_{\chi_1}(s) = \left(\Phi_{\chi_1}(s)\right)^k = \left(\frac{m}{m+s}\right)^{mk}. \tag{95}$$

Taking the inverse Laplace transform of the characteristic function, we get the pdf of the sum defined in Equation (93), or

$$\mathrm{f}_{\chi_k}(\chi_k) = \frac{m^{km}}{\Gamma(km)}(\chi_k)^{km-1}\exp\{-m\chi_k\} \text{ for } \chi_k > 0. \tag{96}$$

The probability of an outage is the probability that χ_k is less than the threshold given in Equation (92); and therefore

$$P_{\bar{\gamma}|k,M}(A_s) = \int_0^{\frac{2^{R_{XY}}-1}{A_s}M^\alpha} \mathrm{f}_{\chi_k}(\chi_k)\partial\chi_k. \tag{97}$$

After integration, this becomes

$$P_{\bar{\gamma}|k,M}(A_s) = 1 - \frac{\Gamma\left(km, \frac{A_s M^{-\alpha}}{2^{R_{XY}}-1}m\right)}{\Gamma(km)}. \tag{98}$$

We use the procedure defined by Equations (75) through (89) and (98) to calculate the outage probability per relay node.

Note that the code rate R_{XY} simply scales the required normalized transmitted signal level. For the calculation of the outage probability per relay node in this Section, the code rate, R_{XY}, is set to 1 (bit/sec/Hz).

For an environment with a relatively large amount of fading (i.e., a Nakagami-m fading factor $m = 0.5$), the performance curves (see Figure 27) suggest that the best communication strategy depends on the desired reliability. If the number of relays is small, such that a fairly large P_ℓ (outage probability) is tolerable, then a simple bucket

brigade ($M = 1$) configuration is marginally best. Lengthening the synthetic waveguide requires smaller outage probabilities P_ℓ to maintain the desired probability of end-to-end link closure, and larger cluster sizes M appear to significantly reduce the required normalized transmitted power.

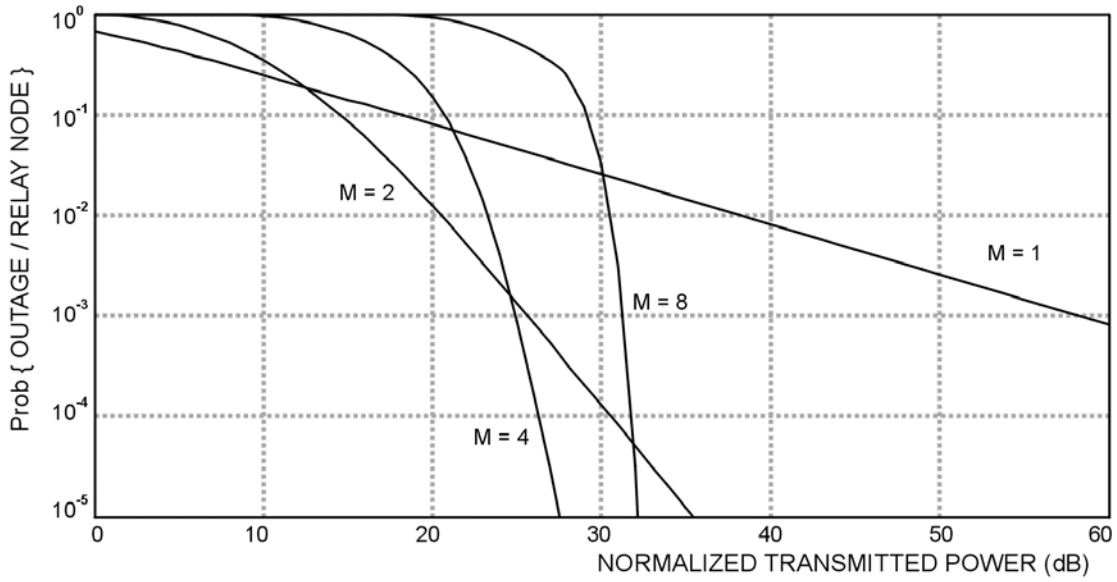

Figure 27. Performance of Space-Time Modulation with a m = 0.5 fading factor

This behavior is attributable to the spatial spreading within the synthetic waveguide, which creates a measure of robustness by allowing the forward flow of packets to effectively bypass individual weak paths. As the cluster size M increases, the minimum required transmit power to effectively cross the increased gap between relay nodes rises, but above this level the increased spatial diversity mitigates the adverse effects of the fading environment.

Figure 28 shows that the normalized transmit power required to reduce the outage probability per relay node to 10^{-2} over a range of fading environments characterized by the Nakagami-m factor. For environments with fading less severe than Rayleigh fading (i.e., $m > 1$) the simple bucket brigade ($M = 1$) is superior, but as fading becomes more severe, increasing the cluster size can greatly reduce the required transmit power.

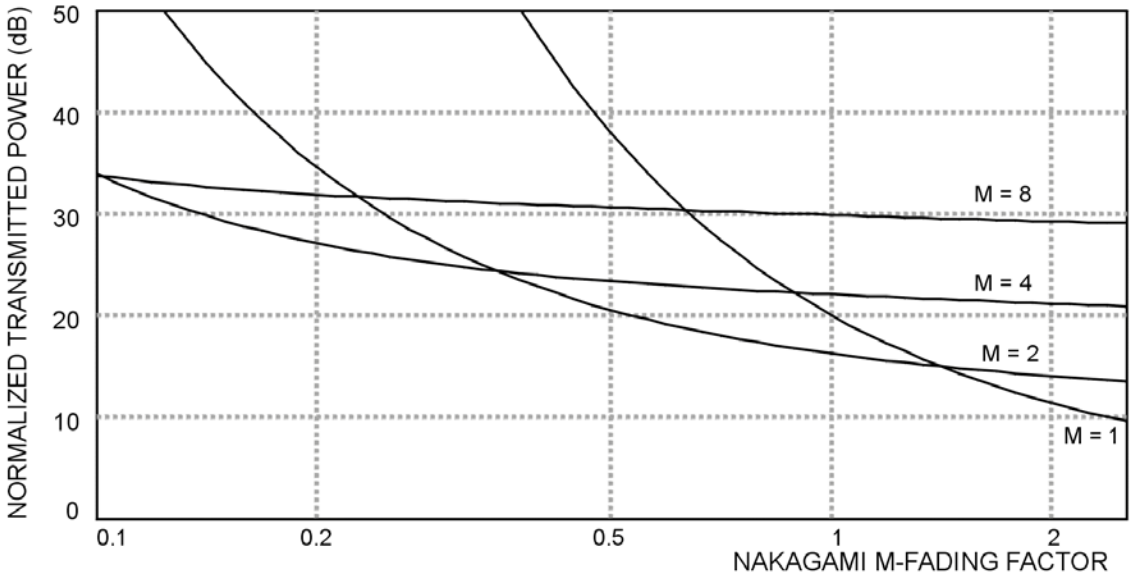

Figure 28. Performance of Space-Time Modulation with $P_\ell = 10^{-2}$

Similarly, the required normalized transmit power for an outage probability per relay node of 10^{-4} is shown in Figure 29. In general, increasing the cluster size of a synthetic waveguide configuration reduces the sensitivity to the amount of fading.

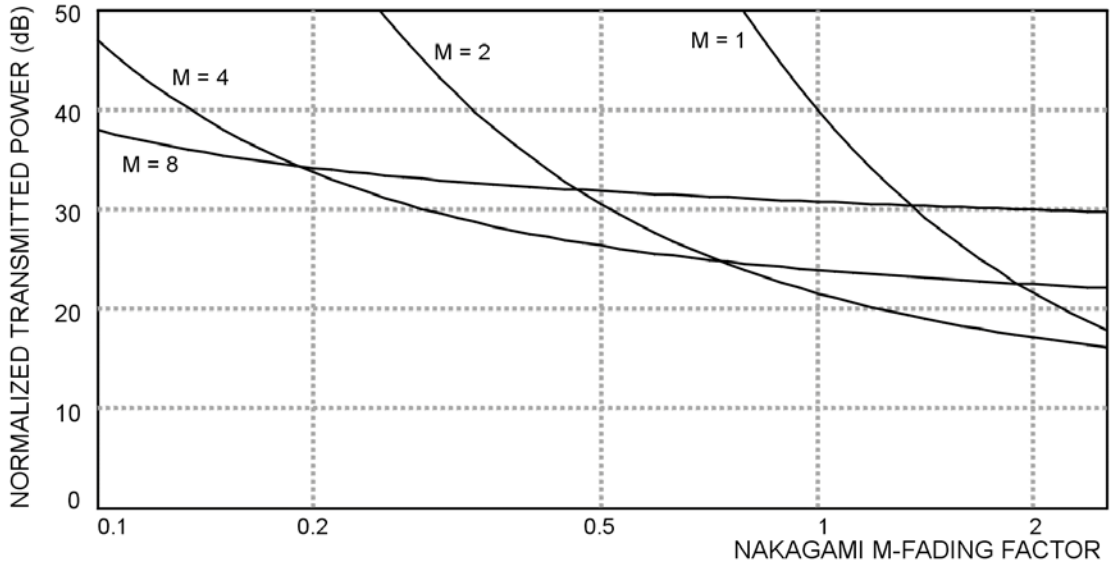

Figure 29. Performance of Space-Time Modulation with $P_\ell = 10^{-4}$

While space-time coding represents a relatively sophisticated modulation technique, the next Section examines perhaps the simplest form of transmit diversity modulation.

B. SIMULCAST MODULATION MODE

The simulcast mode of modulation is where each relay node within a cluster transmits the identical waveform to the adjacent cluster. Each relay node is not necessarily assigned an index within the cluster, and each relay node is not aware of the number of nodes within its cluster that received the source message correctly. The demodulation process treats the aggregate of signals received as if only one signal was transmitted.

With simulcast modulation, a given relay node within the synthetic waveguide receives the sum of the waveforms transmitted from the relay node within the previous cluster. These signals sum noncoherently on the antenna of the relay node resulting in the received signal envelope r_s where

$$r_s \triangleq \left| \sum_{m'=0}^{k-1} r_{m'} \exp\left(j \phi_{m'} \right) \right| \tag{99}$$

for k of M transmitting relay nodes.

If the coding and demodulation scheme recovers the packet without error whenever the coding rate is below the instantaneous channel capacity due to fading, then the probability of outage in this case is

$$P_{\bar{\gamma}|k,M}\left(A_s\right) = \Pr\left\{ R_{XY} > \log_2\left(1 + A_S\, M^{-\alpha} r_s^2\right) \right\} . \tag{100}$$

Rearranging sides of the inequality, we obtain

$$P_{\bar{\gamma}|k,M}\left(A_s\right) = \Pr\left\{ \frac{2^{R_{XY}} - 1}{A_s} M^{\alpha} > r_s^2 \right\} . \tag{101}$$

The pdf for the resultant envelope of the noncoherently summed signal is derived using the circularly symmetric characteristic functions approach that is described in [25] and [26]. The pdf for the received envelope is given by

$$\mathrm{f}_{r_s}\left(r_s\right) = r_s \int_0^{\infty} \rho\, \mathrm{J}_0\left(r_s\, \rho\right) \Lambda_{r_s}\left(\rho\right) \partial\rho \tag{102}$$

where $\Lambda(\rho)$ is the circularly symmetric characteristic function [26], which is defined as

$$\Lambda_{r_s}\left(\rho\right) \triangleq \mathrm{E}_{r_1 \ldots r_K} \left\{ \prod_{i=1}^{K} \mathrm{J}_0\left(\rho r_i\right) \right\} . \tag{103}$$

In this situation, the impinging signals experience independent fading according to the same distribution; therefore,

$$\Lambda_{r_s}(\rho) = \prod_{i=1}^{K} \mathrm{E}_{r_i}\left\{J_0(\rho r_i)\right\} = \Lambda_r(\rho)^K \tag{104}$$

where

$$\Lambda_r(\rho) \triangleq \mathrm{E}_r\left\{\mathrm{J}_0(\rho r)\right\}. \tag{105}$$

An outage occurs whenever the received signal envelope r_s falls below the threshold given in Equation (107) (also see Equation (101)); therefore

$$P_{\bar{\gamma}|k,M}(A_s) = \int_0^T \mathrm{f}_{r_s}(r_s)\,\partial r_s \tag{106}$$

where

$$T \triangleq \sqrt{\frac{2^{R_{XY}}-1}{A_s} M^{\alpha}}. \tag{107}$$

Substituting Equation (102) into Equation (106), we get

$$P_{\bar{\gamma}|k,M} = \int_0^T r_s \int_0^{\infty} \rho\, \mathrm{J}_0(r_s\rho)\Lambda_{r_s}(\rho)\,\partial\rho\,\partial r_s \tag{108}$$

$$= T\int_0^{\infty} \rho\, \mathrm{J}_1(T\rho)\Lambda_{r_s}(\rho)\,\partial\rho. \tag{109}$$

The circularly symmetric characteristic function for a Nakagami-m faded envelope is

$$\Lambda_r(\rho) = \int_0^{\infty} \mathrm{J}_0(\rho r)\,\mathrm{f}_{\mathrm{naka\_m}}(r)\,\partial r. \tag{110}$$

Using the definition from [27]

$$\mathrm{J}_0(x) \triangleq \tfrac{1}{2\pi}\int_0^{2\pi} \exp\left(-jx\cos(\theta)\right)\partial\theta \tag{111}$$

we get the following double integral

$$\Lambda_r(\rho) = (m)^m \big/ m\Gamma(m) \int_0^{\infty}\int_0^{2\pi} r^{2m-1} \exp\left(-mr^2 + jr\rho\cos(\theta)\right)\partial\theta\,\partial r, \tag{112}$$

which is recognized as a form of the Kummer confluent hyperbolic geometric function

$$\Lambda_r(\rho) = {}_1\mathrm{F}_1\left(m,1,-\frac{\rho^2}{4m}\right) \tag{113}$$

where (see [27])

$${}_1\mathrm{F}_1(a,b,z) \triangleq \sum_{k=0}^{\infty} \frac{(a)_k}{(b)_k}\frac{z^k}{k!} \tag{114}$$

and Pochhammer's symbol is defined as

$$(a)_k \triangleq \frac{\Gamma(a+k)}{\Gamma(a)}. \tag{115}$$

The Kummer transformation from [27],

$${}_1\mathrm{F}_1(a,b,z) = e^z\ {}_1\mathrm{F}_1(b-a,b,-z) \tag{116}$$

prevents the numerically unstable summation involving the alternating signs in Equation (113) for $m < 1$.

Combining these results, we get the outage probability at a given relay unit as

$$P_{\bar{\gamma}|k,M}(A_S) = T\int_0^\infty \mathrm{J}_1(T\rho)\exp\left(-\frac{\rho^2}{4m}\right)\left[{}_1\mathrm{F}_1\left(1-m,1,\frac{\rho^2}{4m}\right)\right]^k \partial\rho \tag{117}$$

for

$$T \triangleq \sqrt{\frac{2^{R_{XY}}-1}{A_s}M^\alpha}\ . \tag{118}$$

Note that as in the case of space-time coded modulation, the code rate R_{XY} simply scales the required normalized transmitted signal level. For each calculation of the outage probability per relay node in this section, the code rate R_{XY} is set to 1 (bit/sec/Hz).

For an environment with a relatively large amount of fading (a Nakagami-m fading factor $m = 0.5$), the performance curves for simulcast modulation are similar to the space-time coded modulation; however, the performance of simulcast is inferior (see Figure 30). This is not surprising since the simulcast modulation requires a far simpler demodulation process than does the space-time coded modulation techniques. Nevertheless the simulcast modulation performs quite well, and for an outage probability per relay unit of 10^{-2} (see Figure 31), the difference between the space-time coded modulation and the simulcast is less than 5 dB for the range of Nakagami-m fading factor examined.

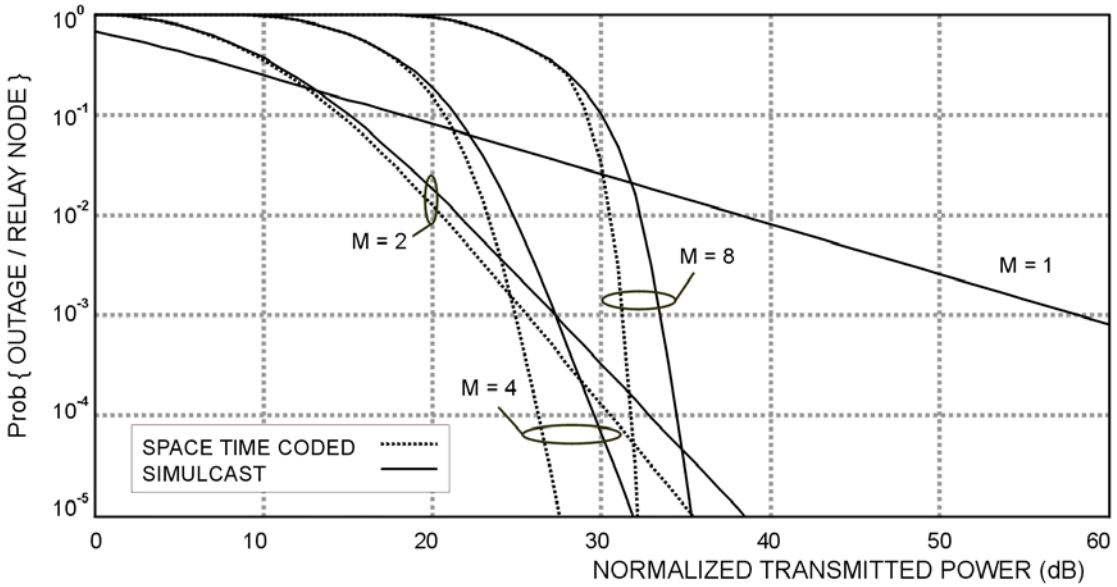

Figure 30. Performance of Simulcast Modulation for a $m = 0.5$ fading factor

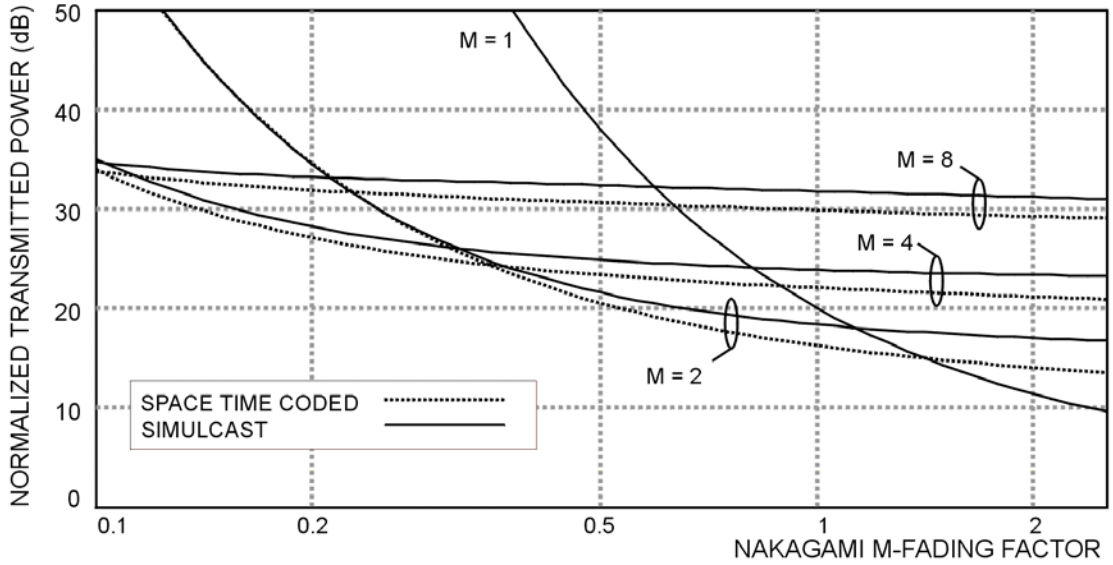

Figure 31. Performance of Simulcast Modulation with $P_\ell = 10^{-2}$

The advantage of the space-time coded modulation becomes much more apparent when the outage probability per relay node is reduced to 10^{-4} (see Figure 32). Interestingly, while one would expect the required normalized signal power to decrease as the channel fading becomes less severe, the required normalized transmitted power actually increases for large Nakagami-m fading factors ($m > 1$). This is likely due to destructive interference among the transmitted signal components.

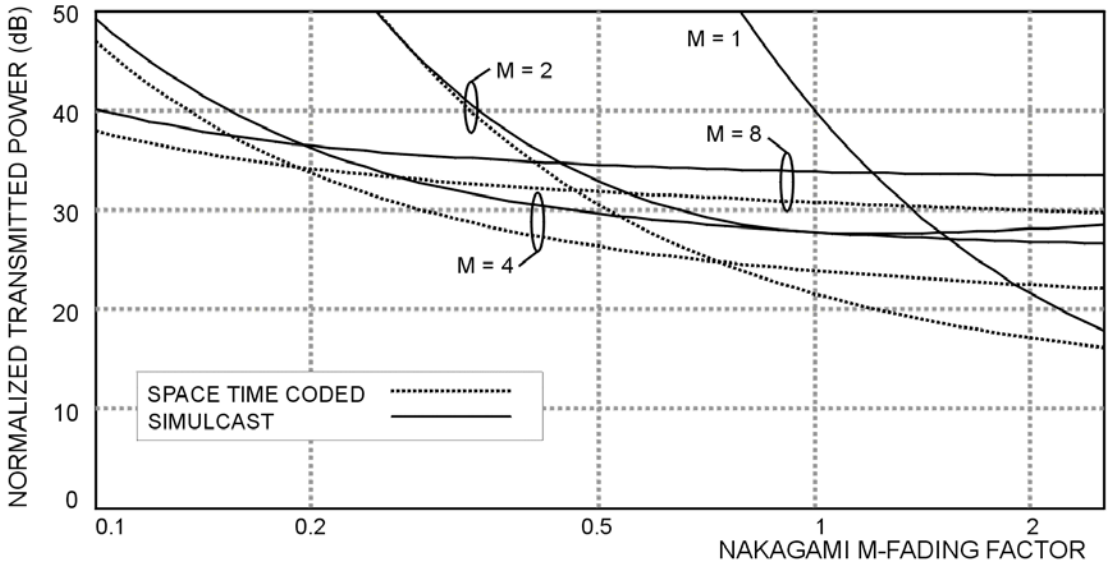

Figure 32. Performance of Simulcast Modulation with $P_\ell = 10^{-4}$

The next section introduces a novel modulation to mitigate this destructive interference, while attempting to maintain the simplicity of the simulcast modulation approach.

C. STUTTERED SIMULCAST MODULATION MODE

The stuttered simulcast mode of modulation is where each relay node within a cluster internally develops the identical waveform, but when transmitted, each relay independently phase modulates the waveform at periodic intervals throughout the transmission of the packet. Each relay node is not necessarily assigned an index within the cluster, and each relay node is not aware of the number of nodes within its cluster that received the source message correctly.

For the ordinary simulcast modulation, Figure 32 indicates that destructive interference limits performance in channels with relatively little fading. The problem is that the waveforms from various transmitting relay nodes arrive with uniformly distributed phase angles, and sometimes the arriving signals cancel each other reducing the signal envelope value on the receiving relay node's antenna. For simulcast modulation, two separate modes of fading are present. The first is due to the ordinary channel fading, and the second is due to this destructive interference among transmitting waveforms. For severe fading, various signal components likely arrive at significantly different power levels, so that the destructive interference is less likely to occur.

The performance in a fading channel can be improved if the block code length extends over many fading coherence time periods. Unfortunately, the channel fading

coherence time is, by definition, greater than a packet length; however, the periods of destructive interference can be reduced. Suppose that the packet frame length is broken into many subframes and each subframe is transmitted on an independently and randomly chosen phase angle by each transmitting relay node. Some subframes within the overall packet will suffer from destructive interference and some subframes will be improved from constructive interference; however, if the block code extends over the entire packet, the averaged performance will prevent a single set of destructive phase rotations from destroying the reception of the entire packet.

In practice, the phase rotation of each subframe need not be truly random, and the receiver could be aware of the set of phase rotation patterns. For coherent data modulation such as BPSK, the length of each subframe must be long enough to allow the receiver to recover the phase rotation in order to realign the subframes to allow for coherent integration across those subframes within the length of the block code.

With stuttered simulcast modulation, a given relay node within the synthetic waveguide receives the sum of the waveforms transmitted from the relay node within the previous cluster. These signal waveforms sum noncoherently on the antenna of the relay node resulting in a transmitted waveform with a received envelope r_s, where

$$r_s \triangleq \left| \sum_{m'=0}^{k-1} r_{m'} \exp\left(j \phi_{m'} \right) \right| \tag{119}$$

for k of M transmitting relay nodes.

However, while the channel fading envelope coefficients r_m, $m = 0,1,\ldots k-1$, remain constant for the duration of the packet, the channel fading phase coefficients ϕ_m are changed every subframe.

If the coding and demodulation scheme recover a packet without error whenever the coding rate is below the instantaneous channel capacity due to fading, then the probability of outage for stuttered simulcast modulation is

$$P_{\overline{\gamma}|k,M}\left(A_s \right) = \Pr\left\{ R_{XY} > \mathrm{E}_{\phi}\left\{ \log_2\left(1 + A_S \, M^{-\alpha} r_s^2 \right) \right\} \right\} \tag{120}$$

where the expectation is over the channel fading phase coefficients, and the probability is taken with respect to distribution governing the channel fading envelope coefficients.

Using the circularly symmetric characteristic function approach described in the previous section, we see that the pdf for the received envelope r_s given the channel fading envelope coefficients r_m, $m = 0,1,\ldots k-1$, is

$$\mathrm{f}_{r_s}\left(r_s \mid r_m, m = 0,1,\ldots k-1 \right) = r_s \int_0^{\infty} \mathrm{J}_0\left(r_s \, \rho \right) \prod_{m'=0}^{k-1} \mathrm{J}_0\left(r_{m'} \, \rho \right) \partial \rho \ . \tag{121}$$

Unfortunately, the integration required in Equation (121) is numerically unstable. Proceeding regardless of this fact, define

$$\underline{r_k} \triangleq \left[r_0, r_1, \ldots, r_{k-1}\right]^T \tag{122}$$

to be a vector containing the channel fading envelope coefficients. Then the probability of outage for the stuttered simulcast modulation mode is given by

$$P_{\overline{\gamma}|k,M}\left(A_s\right) = \int_{\underline{r_k}} \mathrm{U}\left[R_{XY} - \int_0^\infty \log_2\left(1 + A_S M^{-\alpha} r_s^2\right) f_{r_s}\left(r_s \mid \underline{r_k}\right) \partial r\right] f_{\underline{r_k}}\left(\underline{r_k}\right) \partial \underline{r_k} \tag{123}$$

where $\mathrm{U}(x)$ is the unit step function.

Note that unlike space-time coded modulation and simulcast modulation, for stuttered simulcast modulation the code rate R_{XY} does not simply scale the required normalized transmitted signal power level.

Monte Carlo simulations were used to calculate the probability of outage for stuttered simulcast modulation mode, because direct numerically integration is unstable (non-convergent). The Monte Carlo simulations consisted of 10,000 randomly chosen channel fading phase coefficients (inner integral of Equation (123)) for each of a 1000 randomly chosen channel fading envelope coefficients.

The estimated outage probability per relay node for stuttered simulcast modulation is shown in Figure 33 at distinct power level values, and these points are connected with straight lines. The outage probability per relay node for the simulcast modulation and the space-time coded modulation are also plotted. Two separate code rates are shown (R = 1 and R = 4), and for space-time modulation and simulcast modulation, the change in code rate simply scales the normalized transmitted power by 11.76 dB. The curves for the two separated code rates are plotted on different x-axis scales such that the curves for the space-time modulation and simulcast modulation coincide for each code rate. The space-time coded modulation is viewed as bounding the best possible performance, while the simulcast modulation represents the simplest possible modulation scheme in terms of receiver complexity. Any other proposed modulation method ought to fall between these performance limits; this area is shaded gray in Figure 33. By overlaying the curves for the two code rates, we can see the change in relative performance of stuttered simulcast modulation with respect to space-time modulations and simulcast modulation.

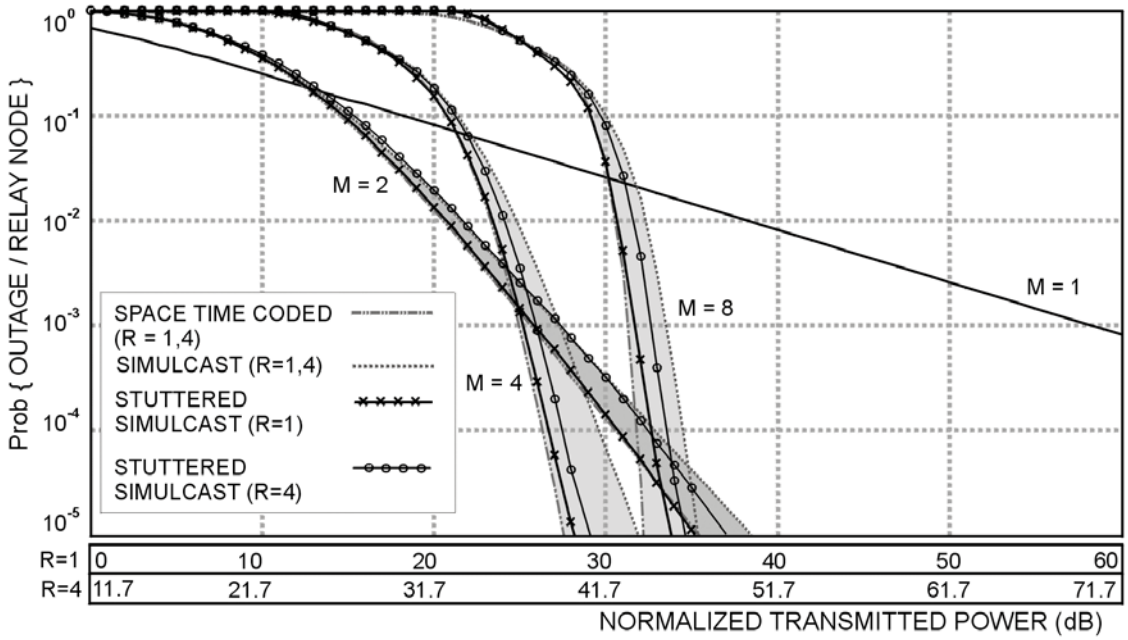

Figure 33. Performance of Stuttered Simulcast for a m = 0.5 fading factor

For the stuttered simulcast modulation with a code rate R_{XY} of 1 (bit/sec/Hz), the performance is very close to the optimal performance provided by the space-time coded modulation. This is significant because a stuttered simulcast demodulator is potentially far less complicated to implement. For the higher code rate of 4 (bit/sec/Hz), the stuttered simulcast performance degrades and becomes similar to the ordinary simulcast. This implies that the stuttered simulcast modulation may only be suitable for low coding rates.

Figure 34 shows the required normalized transmit power to reduce the outage probability per relay node to 10^{-2} over a range of fading environments characterized by the Nakagami m-factor. The point values for the stuttered simulcast modulation with a code rate of 1 (bit/sec/Hz) were estimated via Monte Carlo simulations, and in Figure 34 these point values are connected by straight lines. The area between the performance of the space-time coded modulation and the simulcast modulation is shaded gray. For the depicted range of Nakagami-m fading factors, the performance of the stuttered simulcast modulation is very close to the optimal performance of space-time coded modulation.

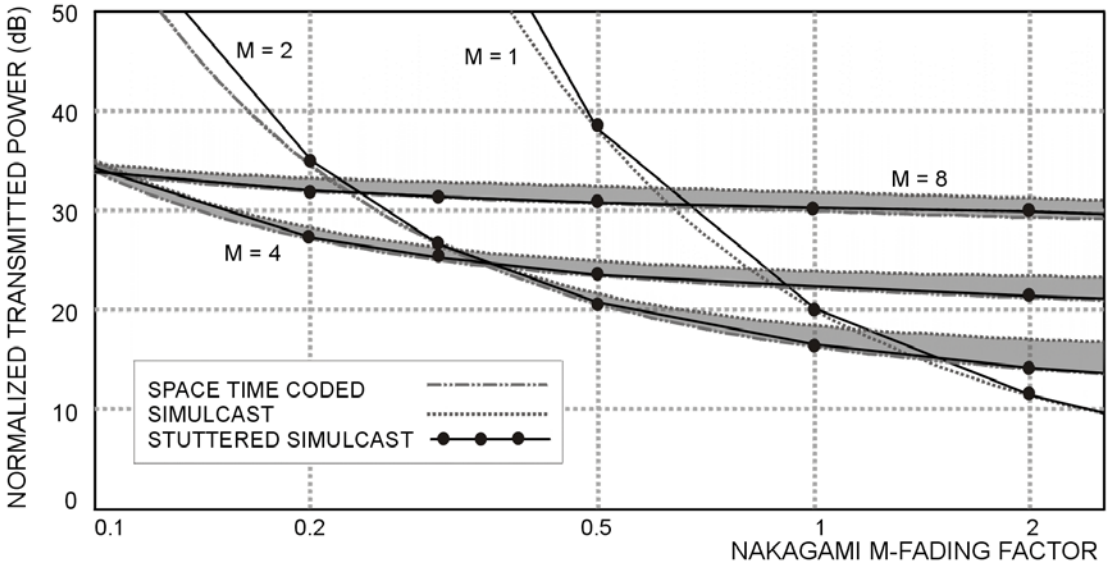

Figure 34. Performance of Stuttered Simulcast Modulation with $P_\ell=10^{-2}$

The near optimal performance of stuttered simulcast modulation with a code rate of 1 (bit/sec/Hz) is maintained when the outage probability per relay node is reduced to 10^{-4} over the same range of fading environments characterized by the Nakagami-m factor (see Figure 35). For a cluster size of two, the performance of the ordinary simulcast modulation degrades with respect to space-time coded modulation as the Nakagami-m fading factor is increased, while the stuttered simulcast modulation continues to track very close to the optimal space-time code modulation's performance.

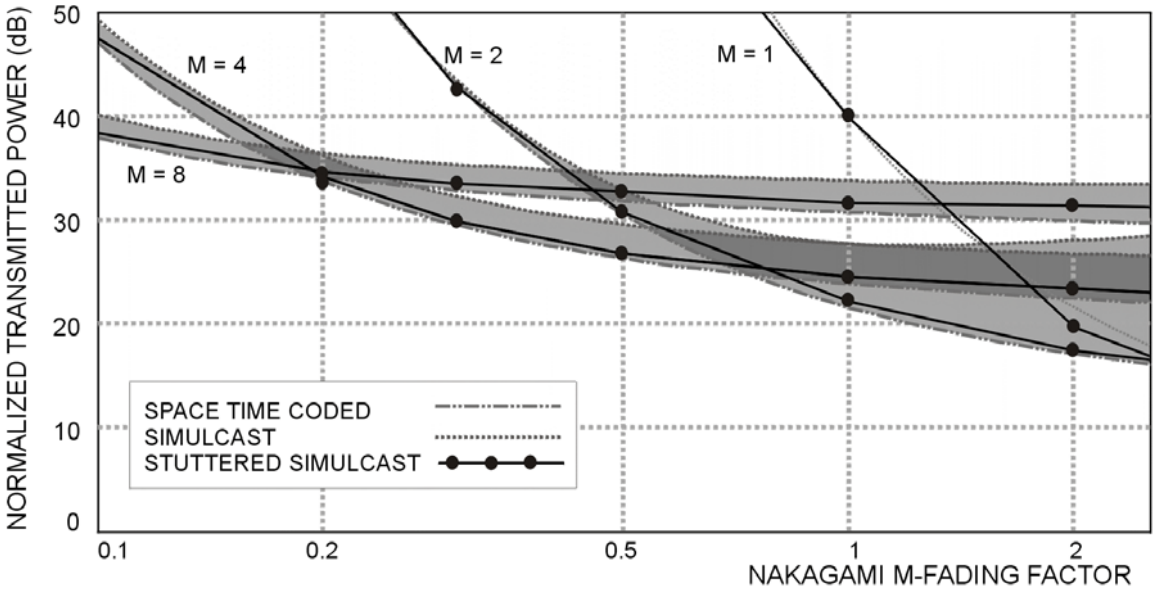

Figure 35. Performance of Stuttered Simulcast Modulation with $P_\ell = 10^{-4}$

The stuttered simulcast modulation appears to provide near optimal performance when operating at a low code rate for all Nakagami-m fading environments. In the next section, the performance of a simulated ad hoc network is compared to the theoretical predicted results developed in this chapter.

D. MONTE CARLO SIMULATION OF THE CODEAN PROTOCOL

A simulation of an ad hoc network using the CODEAN routing protocol, which is described in Chapter II, was developed using the C++ programming language. Within this over 8000-line simulation, relay nodes are randomly dispersed into an area according to a uniform two-dimensional Poisson process. Each set of randomized relay node positions is called a configuration. A set of random channel fading coefficients is drawn according to the environmental channel model, which is described in Chapter II, for the channel between every pair of nodes. A source node and sink node are inserted at a fixed position on opposite end of the ad hoc network field. The source node broadcasts a ROUTE_REQUEST packet, and the nodes within the relay field autonomously process various messages to establish a route to the sink node. The route is successfully established whenever the ROUTE_REPLY message propagates back to the source node, and then a series of DATA packet are sent to the sink node. For each DATA packet, the channel fading coefficients are redrawn according to the appropriate distributions. The

probability of end-to-end link closure (see Equation (88)) is estimated from the number of DATA packets arriving at the sink node

The routing for the bucket brigade configuration consistently required 18 hops given the density of the relay field and the nominal transmitted signal power used during the route set-up process. The number of nodes used in the set-up and the estimated probability of end-to-end closure drove the estimation of the probability of outage per relay node. This outage probability was averaged over many different route set-ups.

For the performance curves shown in this section, the estimated outage probability was averaged over independent 100 configurations of the relay nodes (each requiring a new routing) and 1000 transmitted DATA packet for each configuration.

The performance of the simulated ad hoc network is compared to the predicted performance of the low latency synthetic waveguide for space-time coded modulation (see Figure 36) and for simulcast modulation (see Figure 37). While the synthetic waveguide model does not account for the random variation in relay node positions, the estimated performance of the cooperative diversity enhanced ad hoc network is similar to the predicted performance of the synthetic waveguide. For space-time coded modulation (see Figure 36), the agreement is quite good for a probability of outage per relay node exceeding 0.01, but for any lower probability of outage per relay, the estimated performance for the simulated ad hoc network appears to decay with a smaller exponential rate. This may be due to the path loss variations imposed by the randomly selected relay positions.

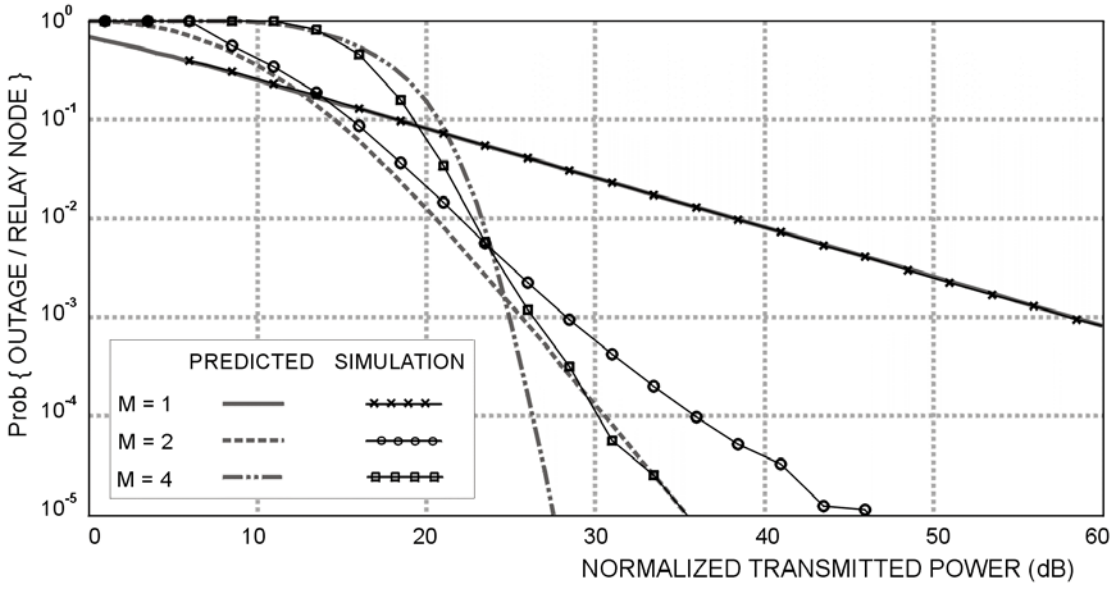

Figure 36. Monte Carlo Simulation of Space-Time Coded Modulation for $m = 0.5$

Curiously, the estimated performance for the simulated ad hoc network appears to perform better than the ideal synthetic waveguide for a normalized power less than 25 dB or so. This phenomenon is likely because, for the cluster size of four, the relay field was traversed in only 4 hops. This low number of hops may be too few for the simulation to settle into the quasi-stationary distribution as modeled in the performance evaluation of the synthetic waveguide

The probability of outage per relay node for simulcast modulation is shown in Figure 37. As in the case of time-space code modulation, the probability of outage per relay node appears to decay at a significantly smaller exponential rate than predicted by the theoretical performance of the synthetic waveguide. To discover the reason for this smaller exponential rate in the tail behavior is certainly worthy of further investigation. For both modes of modulation, increasing the cluster size over the bucket brigade configuration substantially reduces the required transmit power per relay node.

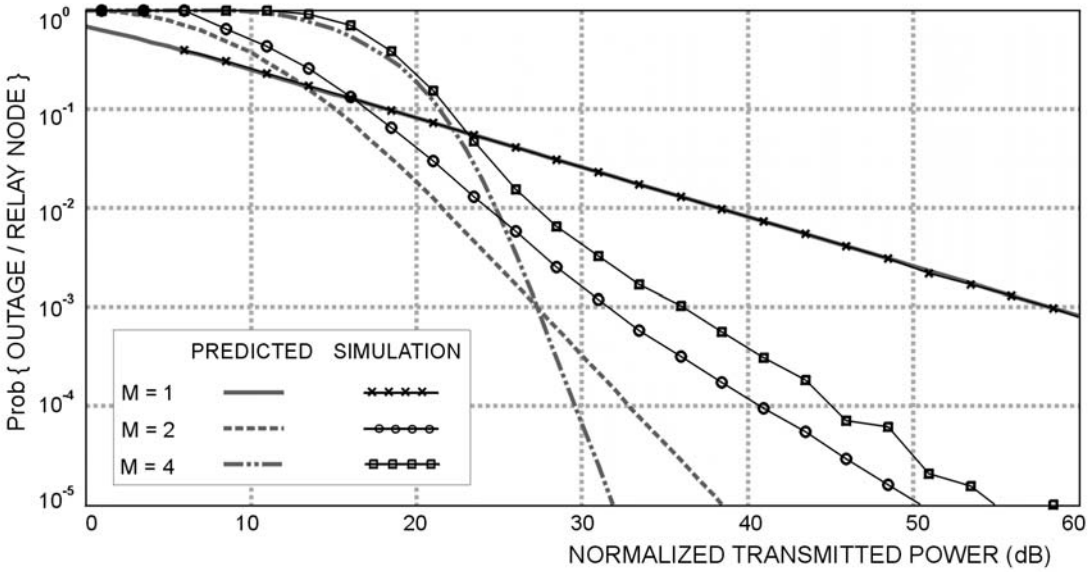

Figure 37. Monte Carlo Simulation of Simulcast Modulation for $m = 0.5$

From Figure 36, if the desired a probability of outage per relay node is 10^{-3} in a Nakagami-m fading environment with a fading factor of $m = 0.5$, then the transmitted power can be reduced by a factor of 30 dB in relation to the power required in a conventional ad hoc network. While the performance estimated using the Monte Carlo simulation of the cooperative diversity enhanced ad hoc network does not quite meet the performance predicted by the theoretical analysis of the synthetic waveguide, the simulation supports the result that incorporating cooperative diversity into ad hoc network protocols can provide a substantial performance improvement.

THIS PAGE INTENTIONALLY LEFT BLANK

V. CONCLUSIONS AND RECOMMENDATIONS

A. CONCLUSIONS

We have introduced a novel communication scheme called "Cooperative Diversity" for creating spatial diversity within an ad hoc network. The performance of a cooperative diversity enhanced ad hoc network was predicted using a simplified structure called the "Synthetic Waveguide." Two modes of operation were examined. For the maximum redundancy mode, the theoretical channel capacity did not predict a substantial advantage in using cooperative diversity. However, for the maximum rate mode, the theoretical channel capacity showed that for higher data throughput rates cooperative diversity outperforms the transitional approaches by creating parallel spatial channels which are jointly robust against severe channel fading.

Next, an outage model was used to evaluate the channel capacity of the synthetic waveguide operating with a realistic low latency restriction in the maximum redundancy mode. The outage model channel capacity result was quite different than that predicted by traditional channel capacity. Whereas traditional channel capacity did not predict a significant advantage in using cooperative diversity technique, the outage model channel capacity demonstrated that for higher data throughput rates cooperative diversity can substantially outperform traditional methods. These results indicate that traditional channel capacity may not be the most appropriate measure to determine the performance of a network of communication devices. To achieve traditional channel capacity requires large blocks of codewords that extend over many channel fading coherence times. While this assumption is often fine for a point-to-point link, within a network consisting of many point-to-point data hops, the resultant latency may quickly become intolerable for practical applications.

A Monte Carlo simulation of the cooperative diversity enhanced ad hoc network reasonably corroborated with the results predicted by the synthetic waveguide. The conclusion is that the cooperative diversity enhanced ad hoc methodology is potentially a very significant improvement over existing ad hoc networking protocols. The cooperative diversity enhanced ad hoc network appears to provide the same throughput performance with the same time-frequency bandwidth requirement using a significantly reduced transmit power level. For example, suppose that 20 relay nodes are selected to deliver data with less than a 0.98 packet error rate (a probability of loss per relay node of

10^{-3}). In a Nakagami-m fading channel with a fading factor of 0.5, the cooperative diversity approach requires 30 dB less transmit power than conventional approaches. In addition, the cooperative diversity enhanced ad hoc network requires far fewer hops reducing the overall communication latency (or delay) across the network.

B. RECOMMENDATIONS

The outage model analysis for the low latency synthetic waveguide only covered the maximum redundancy mode. More research is required to complete this analysis for the maximum rate node of operation under a similar low latency restriction.

An improved channel capacity analysis would include the effects of spatial correlation among links joining adjacent clusters of relay units. Such correlation would likely curtail some of the performance gain demonstrated here especially for a large number of relay units per cluster.

A closer examination of the tail behavior for the probability of outage performance of the cooperative diversity enhanced ad hoc network is required.

The CODEAN protocol requires more throrough investigation to prove that erroneous system states cannot persist. Also, other styles of protocols, such as multicast, that support cooperative diversity techniques require development.

While the theoretical performance of distributed space-time coding was evaluated, actual distributed space-time codes that achieve such predicted performance need to be created and tested.

LIST OF REFERENCES

[1] T. S. Rappaport, *Wireless Communication: Principles & Practice*, Prentice-Hall, Inc., Englewood Cliffs NJ, 1996

[2] M. Weiser, "The computer for the 21st Century," *Scientific American*, Vol. 265, No. 9, pp. 66 – 75, September 1991

[3] C.E. Perkins and E. M. Royer, "Ad-Hoc On-Demand Distance Vector Routing," *Proceedings of 2nd IEEE Workshop on Mobile Computing Systems and Applications*, pp. 90 – 100, New Orleans LA, February 1999

[4] W. Stallings, *Data and Computer Communications (5th Edition)*, Prentice-Hall, Inc., Upper Saddle River NJ, 1997

[5] N.F. Maxemchuk, "Dispersity routing," *Proceedings of ICC '75*, Sec. 41, pp. 10-13, San Francisco CA, June 1975

[6] V.D. Park and M.S. Corson, "A Highly Adaptive Distributed Routing Algorithm for Mobile Wireless Networks, " *Proceedings of INFOCOM '97*, Vol. 3, pp. 1405 – 1413, April 1997

[7] M.S. Corson and A. Ephremides, "A distributed routing algorithm for mobile wireless networks, " *ACM/Baltzer Wireless Journal*, Vol. 1, No. 1, pp. 61-81, February 1995

[8] D.B Johnson and D.A. Matlz, "Dynamic Source Routing in ad hoc networks," *Mobile Computing*, Kluwer Academic Publishers, pp. 153-181, 1996

[9] C.E. Perkins and P. Bhagwat, "Highly Dynamic Destination-Sequence Distance Vector routing (DSDV) for mobile computers", *Proceedings of SIGCOMM '94, Conference on Communications Architectures, Protocols and Applications*, pp. 234-244, August 1994

[10] M. A. Tope, "An investigation of whether diversity enhancement using mobile signal relays increases system-wide capacity," Internal Department of Defense Report, March 1997 (unpublished)

[11] M. A. Tope and J. C. McEachen, "Performance evaluation of synthetic waveguide communication in a Nakagami-m fading environment," *Proceedings of the IEEE Military Communications Conference: MILCOM 2000*, pp. 1154 – 1158, Los Angeles, October 2000

[12] M. A. Tope and J. C. McEachen, "Low-power multipoint relay of tactical communications in a fading enviroment with interference," *Proceedings of the IEEE Military Communications Conference: MILCOM 1999*, Vol. C2, pp. 459 – 462, Atlantic City NJ, November 1999

[13] T. M. Cover and J. A. Thomas, *Elements of Information Theory*, John Wiley & Sons, Inc., New York, 1991

[14] G. J. Foschini and M. J. Gans, "On Limits of Wireless Communications in a fading environment when using multiple antennas," *Wireless Personal Communications*, Vol. 6, pp. 311-335, 1998

[15] A. J. Goldsmith and P. P. Varaiya, "Capacity of fading channels with channel side information," *IEEE Transactions on Information Theory*, Vol. 43, No. 6, pp. 1986 – 1992, November 1997

[16] R. J. McEliece and W. E. Stark, "Channels with block interference" *IEEE Transactions on Information Theory*, Vol. IT-30, No. 1, pp. 44 – 53, January 1984

[17] Abbas El Gamal and Thomas M. Cover, "Multiple user information theory," *Proceedings of the IEEE*, Vol. 68, No. 12, pp. 1466 – 1483, December 1980

[18] S. M. Alamouti, "A simple transmit diversity technique for wireless communications," *IEEE Journal of Selected Areas in Communications*, Vol. 16, pp. 1451-1458, Oct. 1998

[19] V. Tarokh, H. Jafarkhani, and A.R. Calderbank, "Space-time block codes from orthogonal designs," *IEEE Transactions on Information Theory*, Vol. 45, pp. 1456-1458, Oct. 1998

[20] Thomas Cover, Abbas El Gamal, and Masoud Salehi, "Mulitple access channels with arbitrary correlation Sources," *IEEE Transactions on Information Theory*, Vol. IT-26, No. 6, pp. 648 – 657, November 1980

[21] Arron D. Wyner, "The common information of two dependent random variables," *IEEE Transactions on Information Theory*, Vol. IT –21, No. 2, pp. 163 – 179, March 1975

[22] H. Minc, *Nonnegative Matrices*, John Wiley & Sons Inc., New York, 1988

[23] Jack H. Winters, "The Diversity Gain of Transmit Diversity in Wireless Systems with Rayleigh Fading," *IEEE Transactions on Vehicular Technology*, Vol. 47, No. 1, pp. 119 – 123, February 1998

[24] J. G. Proakis, *Digital Communications (3rd Edition)*, p. 35, McGraw-Hill, 1995

[25] C. W. Helstrom, "Distribution of the envelope of a sum of random sine waves and Gaussian noise," *IEEE Transactions on Aerospace and Electronic Systems*, Vol. 35, No. 2, pp. 594 – 601, April 1999

[26] A. Abdi, H. Hashemi, and S. Nader-Esfahani, "On the PDF of the sum of random vectors," *IEEE Transactions on Communications*, Vol. 48, No. 1, pp. 7 – 12, January 2000

[27] M. Abramowitz and A. Stegun, *Handbook of Mathematical Functions*, Dover Publications, Inc., New York, 1972

THIS PAGE INTENTIONALLY LEFT BLANK

INITIAL DISTRIBUTION LIST

1. Defense Technical Information Center
   Fort Belvoir, VA

2. Dudley Knox Library
   Naval Postgraduate School
   Monterey, California

3. Commanding Officer, Naval Information Warfare Activity
   Fort George G. Meade, MD

4. Director, CNO Strategic Studies Group
   Newport, RI

5. Chairman, Code EC
   Department of Electrical and Computer Engineering
   Naval Postgraduate School
   Monterey, California

6. Professor John McEachen, Code EC/Mj
   Department of Electrical and Computer Engineering
   Naval Postgraduate School
   Monterey, California

7. Professor Clark Robertson, Code EC/Rc
   Department of Electrical and Computer Engineering
   Naval Postgraduate School
   Monterey, California 93943-5121

8. Department of Defense
   R531
   Fort George G. Meade, MD

9. Office of Naval Research
   Arlington, VA

10. SPAWAR Systems Center
    D855
    San Diego, CA

11. Naval Information Warfare Analysis Center
    Washington, DC